Hydrogen adsorption on the β-N-covered W(100) surface: An infrared study of the W—H stretch

D. M. Riffe* and A. J. Sievers
Laboratory of Atomic and Solid State Physics and Materials Science Center, Cornell University, Ithaca, New York 14853-2501

(Received 16 May 1989; revised manuscript received 27 September 1989)

The adsorption of hydrogen on the $c(2\times2)$ β-N-covered W(100) surface has been studied with infrared and thermal-desorption spectroscopies. A new dipole-active vibrational absorption due to chemisorbed hydrogen has been discovered. Its center frequency (1738 cm^{-1} for minimal H_2 adsorption), isotopic dependence (1252 cm^{-1} for D_2 adsorption and the existence of both lines for HD adsorption), absorption strength versus β-N coverage, and effective dynamic charge $e^*/\epsilon_\infty \geq 0.12e$ lead to the assignment of the W—H stretch associated with a top-bonded H species. The vibration has been studied in detail on the highly ordered surface characterized by a β-N coverage of 0.5 monolayer: In the zero-coverage limit vibrational decay due to electron-hole pair excitations may provide the dominant contribution to the full width at half maximum of 12 cm^{-1}. Away from this limit inhomogeneous broadening, caused by coadsorption of molecular and other atomic species, appears to increasingly contribute to the width, which attains a maximum of 35 cm^{-1} at saturation. Isotopic dilution and H-coverage experiments reveal a dynamical shift of $+14$ cm^{-1} in going from the isolated adatom to full layer limit which is explained by a combination of direct dipole-dipole and indirect electron-mediated interactions. With increasing coverage two chemical shifts have also been discerned: a positive one ($+21$ cm^{-1}) attributed to electron-density competition among the adsorbed atomic species and a negative one (-17 cm^{-1}) due to molecular-species coadsorption. Low-temperature annealing produces an increase in barrier height to parallel motion from the on-top site, apparently caused by the filling of more tightly bound sites near the remaining on-top H. The concurrent constancy of the W—H vibrational frequency indicates that the potential well perpendicular to the surface is not drastically altered by this rearrangement of adatoms.

I. INTRODUCTION

Among the plethora of surface-science techniques which have been used to investigate transition-metal-surface–H systems, the vibrational probes of electron-energy-loss spectroscopy (EELS) and infrared reflection-absorption spectroscopy (IRAS) have been particularly productive in discerning the nature of the H adlayer. EELS, e.g., has been instrumental in identification of the H-adatom site through a measure of the adsorbed-H-atom normal-mode frequencies. Beyond this both EELS and IRAS have provided essential information on the intra-adlayer and adlayer-metal coupling mechanisms through determinations of vibrational linewidth, line shape, and center-frequency shifts upon increasing coverage and/or isotopic dilution. A general feature of H chemisorption which has emerged from these studies is that the H atom prefers to be multiply coordinated, residing in fourfold, threefold, or bridge-bonded sites.[1] Additionally, it seems for these sites that the dynamic coupling between adsorbed-H oscillators is dominated by substrate-mediated electronic interactions.[2–4] Absent though, from the accumulated data set, is evidence for a simply coordinated top-bonded-H species even though single-metal-atom–H bonds are known to exist in various transition-metal hydride complexes[5] and for H bonded to alumina-supported metal particles.[6]

In the present paper we present a study of hydrogen adsorption on a modified transition-metal surface: W(100) covered by submonolayer atomic nitrogen, henceforth designated β-N/W(100). Using infrared reflection-absorption spectroscopy the first example of the elusive single-metal-atom-bonded H species in a macroscopic metal-surface environment has been detected and further studied as a function of H coverage, β-N coverage, temperature, and isotopic-H concentration. We find that the W—H symmetric-stretch vibration is characterized by a dynamic charge of $e^*/\epsilon_\infty \geq 0.12e$ with a zero-coverage-limit center frequency of 1738 cm^{-1} and linewidth of 12 cm^{-1}. Although electron-hole pair excitations may account for the linewidth at zero coverage, inhomogeneous broadening appears to dominate away from this limit resulting in a saturation coverage linewidth of 35 cm^{-1}. Additionally, as the coverage is increased, two chemical interactions contribute to a shift in center frequency: a positive one due to electron-density competition by the adsorbed atomic species and a negative one caused by molecular coadsorption. A positive dynamical shift has also been measured. In contrast to previously studied monolayer-regime H layers,[2–4] the indirect electronic coupling of the H oscillators is significantly augmented by the direct dipole-dipole interaction.

Concurrent thermal-desorption (TD) spectra have also been used to elucidate the nature of the on-top H as well as other hydrogen species on the β-N/W(100) surface. Two above-room-temperature (RT) peaks as well as three

 ©1990 The American Physical Society

below-RT features (one of which is from molecularly adsorbed hydrogen) have been discerned in the desorption of hydrogen from the β-N/W(100) surface. However, none of these features can be associated with direct desorption from the on-top sites. Rather, heating the 100-K surface results in the migration of the on-top to other more tightly bound sites which, in turn, tends to block further migration from the on-top sites.

After a brief description of the experimental details in Sec. II, the experimental results are presented in Sec. III in four subsections. Low-energy electron diffraction (LEED) observations of the β-N-covered W(100) surface are first described (Sec. III A) since they are useful in locating the most highly ordered β-N coverage of 0.5 monolayer (ML) where most of the ir measurements have been made. Since there have been no previous low-temperature investigations of hydrogen and nitrogen coadsorption on W(100), a detailed presentation of the ir and TD results takes place in the rest of Sec. III. A delineation of the changes in the ir and TD spectra which occur as the β-N coverage grows from zero to 0.5 monolayer is presented in Sec. III B. The ir experiments done on the highly ordered 0.5-ML β-N surface are then detailed in Sec. III C which describes H_2, D_2, and HD spectra at saturation, results versus H_2 coverage, low-temperature annealing experiments, and isotopic-dilution data.

Discussion of the results occurs in Sec. IV. After identification as belonging to an atomically adsorbed species and consideration of six binding sites (all of the possible sites with at least one mirror plane) the 1738-cm^{-1} vibration is assigned to the W—H stretch associated with an H atom bonded to one surface-W atom (Sec. IV A). This vibrational mode is then used as a probe of the underlying β-N (Sec. IV B). Section IV C examines possible contributions to the linewidth. The isotopic-dilution frequency shifts are used to help extricate the static and dynamic contributions to the center-frequency shift with increasing H coverage in Sec. IV D. A discussion of surface potentials for hydrogen adlayer follows in Sec. IV E. Lastly, the conclusions for H adsorption on β-N/W(100) are summarized in Sec. V.

II. EXPERIMENTAL DETAILS

In the present IRAS setup[7] an $f/10$ beam of broadband radiation from a Nernst glower is focused through a CsI window onto the crystal at a mean angle of incidence $\theta=84°$. The light then exits the UHV chamber and is steered through a linear polarizer (to eliminate the *s*-polarized component) and into the emission port of a Bomen DA3 Fourier-transform interferometer spectrometer where it is modulated (4 cm^{-1} resolution for all data in this study) before striking a narrow band (900–5000 cm^{-1}) Hg-Cd-Te photoconductive detector. In order to minimize the effects of atmospheric water-vapor lines on the spectra, all sections of the beam path are either under vacuum or are purged with dry N_2.

The sample is the same W(100) crystal ($6.1\times0.6\times0.17$ cm^3) used in previous infrared surface-electromagnetic-wave (SEW) investigations.[8,9] Details of the sample environment are essentially the same as for those studies except that the crystal holder is now mounted on the bottom of a liquid-N_2-cooled cryostat which provides an ultimate base temperature of ~88 K. (Temperature is measured with a W–26 at. % Re/W–5 at. % Re thermocouple spotwelded to the top edge of the crystal near the center of its longest dimension.) Upon reinsertion into the UHV chamber after the SEW studies and prior to any IRAS measurements, the sample was baked in 10^{-7} Torr of O_2 for ~5 h at 1520 K with periodic flashes to 2300 K. This treatment reestablished the low-temperature, clean surface $c(2\times2)$ LEED pattern, indicating that the surface was devoid of any C contamination.[10]

Before each experimental run the sample is again flashed to 2300 K after which it cools to room temperature in ~7 min; it is then exposed to N_2. Except where noted below, the sample is subsequently annealed to 900 K for 60 sec in order to produce a $c(2\times2)$ β-N/W(100) surface with minimal disorder (see Sec. III A). Upon cooling to 100 K two reference spectra are taken. (The base pressure of the chamber is such that only ~7% of a monolayer of H is adsorbed by this time.) This is followed by H_2 exposure of the crystal and then two more ir spectra.

Thermal-desorption spectra are measured by monitoring the partial pressure of any particular mass with a quadrupole mass spectrometer. Additionally, the infrared optical geometry is arranged so that LEED observations can be made simultaneously with the collection of the ir data.

III. EXPERIMENTAL RESULTS

A. $c(2\times2)$-β-N LEED

Since the H absorption under scrutiny exists only in the presence of β-N, LEED observations of this phase are briefly described before delving into the ir and TD results. Previous LEED (Refs. 11 and 12) along with EELS (Ref. 13) studies have determined that at RT the N_2 molecule breaks apart with each N atom occupying a fourfold hollow site resulting in a state which is termed β-nitrogen. At all β-N coverages $\frac{1}{2}$-order $c(2\times2)$ spots are apparent although without annealing they remain rather broad and fuzzy. Annealing to 900 K (for 60 sec in the present study) has the effect, for coverages $>\sim0.3$ ML of producing more order in the β-N layer resulting in sharper $\frac{1}{2}$-order beams. For $\theta_{\beta\text{-N}}=0.5$ the half-order spots are sharpest upon annealing, which has resulted in the interpretation that the surface is highly ordered with atomic N adsorbed in every other fourfold hollow site along the ⟨10⟩ directions.[11] Further adsorption leads to a saturated RT coverage of $\theta_{\beta\text{-N}}=0.6$ ML.[14]

The present LEED data are in general agreement with previous studies[11–12,15] and are summarized in Table I. For the exposures shown, it is evident that ~0.4 langmuir (L) (with 1 $L\equiv10^{-6}$ Torr sec) produces a layer which is closest to $\theta_{\beta\text{-N}}=0.5$. These LEED results, along with ir data, are used in the next section to more accurately assign a coverage of $\theta_{\beta\text{-N}}=0.5$ ML to an exposure of 0.41 L.

TABLE I. β-N LEED changes upon 900-K anneal.

Exposure (L)	$c(2\times2)$ $\frac{1}{2}$-order spots after 900-K anneal
≤ 0.2	Still fuzzy, no apparent change
0.25–0.35	Sharper than ≤ 0.2 L exposure but less sharp than integral-order spots
0.38–0.42	Sharpest, same as integral-order spots. Also sharp, faint $p(2\times1)$ $\frac{1}{2}$-order spots.
0.45	Not as sharp as 0.4 L exposure. Faint $\frac{1}{5}$-order spots around both integral- and $c(2\times2)$ $\frac{1}{2}$-order spots.
≥ 0.50	Sharp with very distinct $\frac{1}{5}$-order spots around both integral- and $c(2\times2)$ $\frac{1}{2}$-order spots.

B. Infrared and thermal desorption versus β-N coverage

After discovery of an infrared absorption in the 1740-cm^{-1} range on the β-N/W(100) surface, verification that it was due to ambient hydrogen was obtained by exposing the β-N/W(100) surface to deuterium, which resulted in a line in the 1260-cm^{-1} range. Following this a more systematic study using ir and thermal-desorption spectroscopies was carried out on β-N/W(100)+H_2 as a function of β-N coverage.

1. Infrared determination of 0.5-ML β-N coverage

Figure 1 (Ref. 16) exhibits the growth of the ir spectrum for a saturation dose of H_2 as β-N coverage is increased up to a maximum near 0.6 ML.[14] Initially there is one line which is fixed at $\sim$1766 cm^{-1} with a width of $\sim$35 cm^{-1}, but as $\theta_{\beta\text{-N}}$ approaches maximum coverage, a second line, which is just a slight shoulder at $\theta_{\beta\text{-N}}=0.5$ ML, becomes distinct at $\sim$1790 cm^{-1}.

The curves in Fig. 1 are labeled by the coverage of the β-N layer which is placed on the W surface before H_2 exposure. The coverages are determined in the following manner.[17] As is evident from Table I, 0.4 L N_2 exposure is quite close to a β-N coverage of 0.5 ML since at that exposure the sharpest $\frac{1}{2}$-order $c(2\times2)$ spots are observed. The LEED pattern, however, is not visually very different for N_2 exposures between 0.38 and 0.42 L. More precise assignment can be obtained with help from a plot of $\int(\Delta R/R_0)d\nu$ for the hydrogen mode versus N_2 exposure which is shown in Fig. 2. As discussed in Sec. IV A, the hydrogen mode at 1766 cm^{-1} is assigned to the perpendicular vibration of H on top of one W atom (i.e., the W—H stretch) in the presence of two nearest-neighbor β-N atoms. [This is in contrast to the clean W(100) surface where hydrogen is solely bridge bonded.] The absorption strength should therefore reach its maximum when each W atom is straddled by two N atoms. The β-N coverage for which this occurs is precisely $\theta_{\beta\text{-N}}=0.5$ ML which, according to the plot in Fig. 2, is equivalent to 0.41 L N_2 exposure. This data point and previously published curves of the carefully studied N_2 sticking coefficient versus coverage[11,14] are then used to assign $\theta_{\beta\text{-N}}$ values to other RT N_2 exposures.

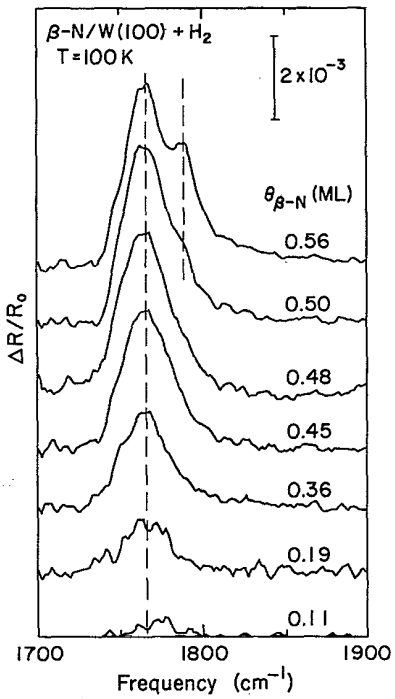

FIG. 1. Change in normalized reflectivity in W—H-stretch region vs $\theta_{\beta\text{-N}}$ for saturated H_2 exposure onto 900-K-annealed β-N/W(100) at 100 K. For $\theta_{\beta\text{-N}}<0.5$ ML only one line is apparent, located at 1766 cm^{-1}. For $\theta_{\beta\text{-N}}=0.56$ ML and to a much lesser extent for $\theta_{\beta\text{-N}}=0.5$ ML there exists a second line at $\sim$1790 cm^{-1}.

We point out that all is not quite perfect with the $\theta=0.5$ ML β-N surface as defined by an exposure of 0.41 L: there exist both β-N-rich and β-N-poor regions for such an exposure. The first evidence of imperfection is

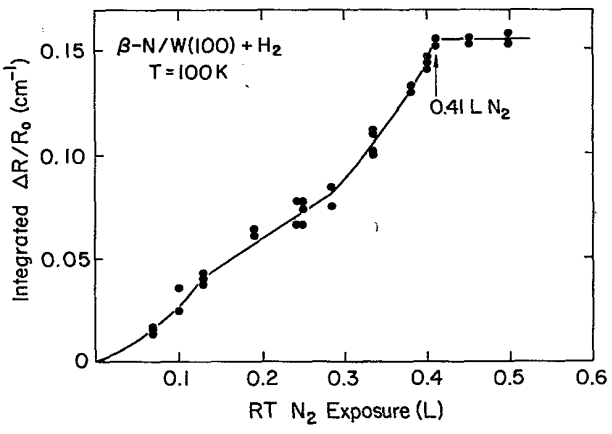

FIG. 2. Integrated $\Delta R/R_0$ of W—H stretch vs RT N_2 exposure (used to produce β-N) for saturated H_2 exposure onto 900-K-annealed β-N/W(100) at 100 K. Note that a sharp break occurs in integrated $\Delta R/R_0$ for a N_2 exposure of 0.41 L. This point is taken to correspond to 0.5 ML of β-N (see text for discussion). The solid line is drawn as a guide to the eye.

the faint, but sharp, $p(2\times1)$ LEED beams apparent in the $c(2\times2)$ pattern. Additional evidence is found in Fig. 1. For $\theta_{\beta\text{-N}}=0.5$ ML (0.41 L N_2 exposure) there exists a high-frequency shoulder on the main absorption peak which turns into a distinct peak by 0.56 ML (=0.5 L N_2 exposure). Hence on the 0.41-L surface there exists some β-N structure associated with coverages higher than 0.5 ML. In contrast, Fig. 3, which is discussed in more detail momentarily, shows the existence of a slight β_1 H_2 TD peak, which is associated with the clean-W surface, on the $\theta_{\beta\text{-N}}=0.5$ ML (0.41 L N_2 exposure) surface. This exposure, however, seems to be the best compromise in minimizing both kinds of defects. It is therefore taken to represent most closely the ideal $\theta_{\beta\text{-N}}=0.5$ ML surface.

2. β-N coverage dependence of the H_2 TD spectrum

Concurrent with the growth of the infrared absorption of Fig. 1 are drastic changes in the H_2 thermal-desorption spectra from the surface. These changes are exhibited in Fig. 3.[18] With greater β-N coverage the clean-surface β_1 and β_2 peaks decrease as three new peaks, marked γ', β_1', and β_2', increase in area.

Also present is another H_2 feature just above γ' which is not associated with the sample. The most noticeable thing about this extra feature is that it exhibits no variation with β-N coverage. This is the first clue that it does not originate from the W crystal. Confirmation of this observation was obtained by varying the sample heating rate and the sample temperature when the *e*-beam current was turned on. For example, the sample can be radiatively heated to RT without the appearance of the peak. Further heating with the electron beam, however, produces this peak with a time lag equivalent to that observed when the *e* beam is used initially from low temperatures. Apparently the electron beam is heating some part of the sample holder (which does not adsorb N_2) which produces this peak above γ'.

Although it is impossible to completely rule out spurious sources as producing the β_1', β_2', and γ' peaks, it seems most likely that these features are from the β-N modified W(100) surface. This is substantiated by two observations. The first is that, aside from the extra low-temperature peak and a small broadband piece (the section between the two dashed curves), the clean-surface ($\theta_{\beta\text{-N}}=0$) H_2-TD β_1,β_2 spectrum is in excellent agreement with previously published curves for H_2/W(100).[19] The second observation is that the clean-surface spectrum smoothly transforms into the $\theta_{\beta\text{-N}}=0.5$ ML spectrum as more N_2 is added to the surface. It seems unlikely that some other nearby surface, which does not adsorb H_2 without preadsorbed nitrogen, would adsorb H_2 in the presence of nitrogen.

As shown in Fig. 4 the total amount of hydrogen adsorbed on the crystal[20] decreases as the quantity of β-N is increased. In this figure, as well as the rest of the figures which show H_2-TD amounts, the amount of H_2 desorbed is in units of monolayers of adsorbed H_2 *molecules* (as is shown below, some of the adsorbed H_2 is in atomic and some in molecular form on the surface). The data for this figure include the curves of Fig. 3 and the scale is set by the clean surface W(100)+H_2 TD curve of Fig. 3 which

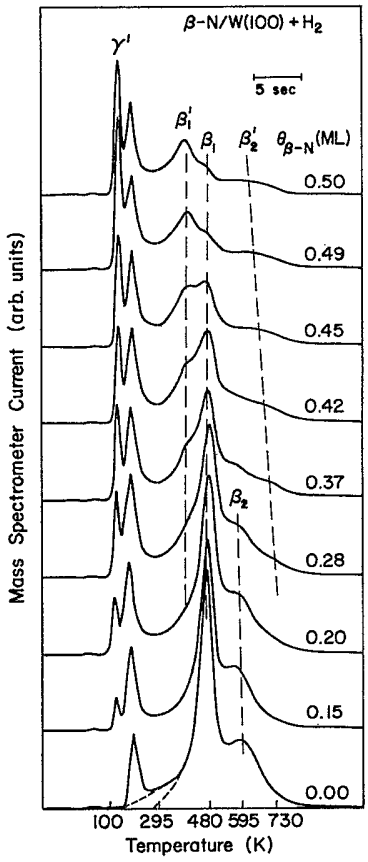

FIG. 3. H_2-TD spectra vs $\theta_{\beta\text{-N}}$. The evolution of the H_2-TD spectrum is displayed as β-N coverage is increased from 0 to 0.50 ML. Concurrent with the disappearance of the clean surface β_1 and β_2 peaks are the appearance of γ', β_1', and β_2' features. Heating rate is 40 K sec^{-1}.

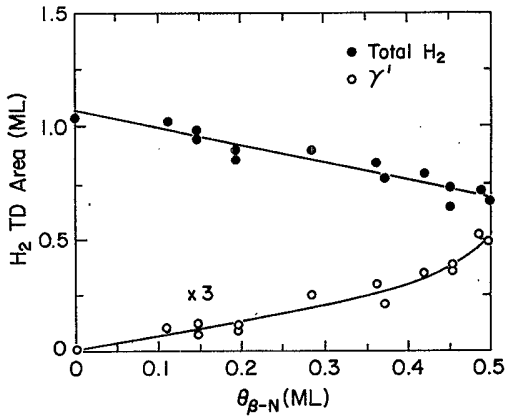

FIG. 4. H_2-TD area vs β-N coverage for saturated H_2 exposure onto 900-K-annealed β-N/W(100) at 100 K. Shown are the total amount desorbed and the amount in the γ' peak for a LT heating rate (with *e*-beam current on) of 40 K sec^{-1}. The total H_2 coverage at $\theta_{\beta\text{-N}}=0.5$ ML is 0.65±0.05 ML. The γ' data has been multiplied by a factor of 3. The solid lines are guides to the eyes.

is known to adsorb 1 ML of H_2 molecules. A value slightly higher than 1 for this curve in Fig. 4 comes from the small extra broadband piece located between the two dashed lines in the clean-surface curve of Fig. 3. The extra nonsample low-temperature peak is eliminated from the measured areas in a manner similar to that shown by the leftmost dashed curve in the bottom trace. These data, along with careful comparisons of other clean-surface and $\theta_{\beta\text{-N}}=0.5$ ML H_2-TD data, lead to the assignment of 0.65 ± 0.05 ML of H_2 desorbed from the 0.5-ML β-nitrogen surface.

Also plotted in Fig. 4 is the amount desorbed in the γ' peak for data including that shown in Fig. 3 where the low-temperature (LT) heating rate is 40 K sec^{-1} (*e*-beam current on).[21] A monotonic increase in the γ' area occurs as β-N coverage increases.

3. *Nature of H_2 thermal-desorption features*

In order to learn whether the γ', β_1', and β_2' TD peaks are from desorbed molecular or atomic species, experiments were performed by adsorbing D_2, H_2, and HD onto a $\theta_{\beta\text{-N}}=0.5$ ML surface. The results are summarized in Table II. Because they are not easily separated, the areas of the β_1' and β_2' are combined in the category "HT peaks." The overall scale of the table is set by assuming a total TD area of 0.65 ML for H_2 adsorption. Sensitivity of the mass spectrometer to the three gases was calibrated from TD spectra taken from saturated W(100) without any N_2 preadsorption by assuming that equivalent amounts of each individually adsorbed isotope saturate the clean W(100) surface.

A peak which comes from randomly associated atomic species should yield, upon HD adsorption, equal amounts of H_2+D_2 and HD. This is close to what is observed for the HT β_1' and β_2' peaks. The slightly larger value of $H_2+D_2=0.23$ ML compared to 0.19 ML for HD is slightly puzzling. Clearly though, these peaks are atomic in nature. As expected, approximately equal amounts of β_1' and β_2' occur for adsorption of any of the isotopes; the slightly larger value of H_2 for H_2 adsorption is attributed to slight ambient adsorption of H_2 for the HD and D_2 runs.

Vastly different behavior is observed in the γ' peak. First, it is not exclusively atomic in nature. In fact, at least $\frac{1}{2}$ of the peak is from desorption of molecular species (assuming that atomic recombination is isotopically random). Also apparent are the *unequal* amounts of total γ' desorption for the three isotopes. Clearly as the mass increases, the γ' area increases. This is perhaps not too surprising for a weakly bound molecular species where zero-point motion can affect the effective well depth. In fact, it is shown at the end of Sec. III C 1 that all the difference in γ' desorption for H_2 and D_2 adsorption is attributable to adsorbed molecular species. It has been similarly observed on the (111) face of W, which also supports molecular H_2 adsorption at low temperatures, that the H_2 isotope is more weakly bound than D_2.[22] It is seen below that this unequal γ' adsorption behavior is key to the understanding of some of the ir results on this system.

In order to more clearly delineate the LT desorption behavior in hopes of correlating it with the ir feature, later TD spectra, whose areas are plotted in several figures which follow, were taken slightly differently. For these spectra the sample was warmed to RT relatively slowly using solely radiation from the filament. An example of one such LT spectrum is displayed in Fig. 5. The extra nonsample peak is now absent (it occurs later when the sample is *e*-beam heated above RT). The γ' peak is now revealed as two peaks, a sharp one followed by a broader one at 126 K for a heating rate of 1.4 K sec^{-1}. Under the assumption of first-order kinetics and a frequency factor of 3×10^{-12} sec^{-1}, a desorption energy of 7.8 kcal/mol is implied by the second peak, a value which is situated in between the two values of 7.6 and 8.1 kcal/mol deduced for the two γ peaks from W(111).[23] However, TD spectra of H_2, HD, and D_2 taken from H_2-D_2 isotopic mixtures indicate that the first sharp peak is from an atomic species but that the broader second peak is actually two unresolved peaks, with the slightly lower-temperature one from molecularly ad-

TABLE II. Thermal desorption areas for H_2, HD, and D_2 adsorption onto $\theta_{\beta\text{-N}}=0.5$ ML β-N/W(100).

Adsorbed gas	Desorbed gas	TD areas (ML) γ'	HT peaks $(\beta_1'+\beta_2')$
H_2	H_2	0.20	0.45
HD	HD	0.19	0.19
	H_2	0.03	0.12
	D_2	0.03	0.11
	$HD+H_2+D_2$	0.25	0.42
D_2	D_2	0.31	0.41

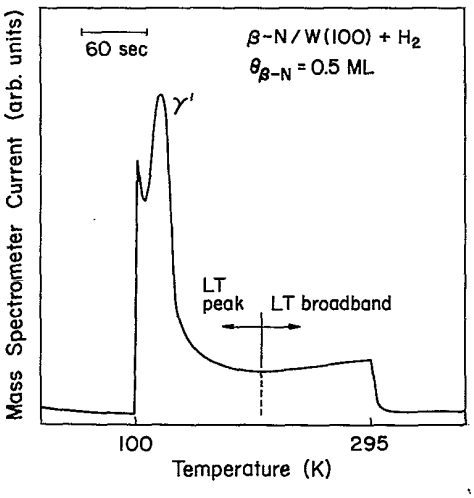

FIG. 5. LT H_2-TD spectrum. For lower heating rates (1.4 K sec^{-1} for spectrum shown) the γ' peak is revealed to be two peaks. For later purposes of analysis the LT spectrum is divided into two sections, LT peak and LT broadband, as illustrated.

sorbed hydrogen and the higher-temperature one again from atomically adsorbed H.

Below RT there is also a rather large broadband section which has a minimum at ~230 K. Somewhat arbitrarily, this minimum is used as the dividing line for what is labeled, in some of the following figures as "LT peak" and "LT broadband." In those same figures "HT peak" refers to the area desorbed above 295 K which includes the β_1' and β_2' features, where again 295 K is a somewhat arbitrary, if not convenient, dividing line. As before, all HT spectra are obtained with the *e*-beam current on.

C. Adsorption onto the well-ordered 0.5-ML β-N surface

1. H_2, D_2, and HD saturation exposure

Figure 6 displays the absorption spectrum of H_2, D_2, and HD at saturation each adsorbed on the $\theta_{\beta\text{-N}}=0.5$ ML, 900-K-annealed surface at 100 K. For H_2 there exists one absorption feature at 1766 cm^{-1} with $\int(\Delta R/R_0)d\nu=0.176\pm0.005$ cm^{-1}. Similarly, D_2 adsorption exhibits one absorption feature at 1264 cm^{-1} with $\int(\Delta R/R_0)d\nu=0.0856\pm0.0025$ cm^{-1}. The small negative feature at 1738 cm^{-1} is due to displacement of ambiently adsorbed hydrogen by the deuterium. HD adsorption, however, yields two absorption features, one at 1264 cm^{-1} with $\int(\Delta R/R_0)d\nu=0.0712\pm0.0025$ cm^{-1} and one at 1753 cm^{-1} with $\int(\Delta R/R_0)d\nu=0.0322\pm0.0015$ cm^{-1}.[24] It is interesting that for HD adsorption the lower-frequency peak is stronger than the higher-frequency peak.

2. ir and thermal desorption versus H_2 coverage

The absorption features for H_2 and D_2 adsorption were measured in greater depth as a function of H_2 exposure. As qualitatively shown in Fig. 7, with increasing H_2 exposure the absorption increases in frequency and becomes broader, with a slight symmetry-breaking tail to the high-frequency side.

In order to more quantitatively explore the coverage-dependent changes, some measure of the on-top coverage (which is responsible for the absorption as discussed in Sec. IV A) is needed. Since there seems to be no one-to-one correspondence between any of the TD peaks and this adsorption site, TD areas are not an adequate measure of the on-top coverage. And because there are at least two states of H_2 adsorption (atomic and molecular) the total TD area is also inadequate. LEED is of no use either since there are no significantly new LEED patterns upon H_2 adsorption which might signify a particular coverage. The only possibility left as an on-top coverage measure is the integrated area of the vibrational absorption feature. Hence, in all of the following figures which have an axis labeled "Fractional On-top Coverage," the values are determined by the ratio $[\int(\Delta R/R_0)d\nu]/[\int(\Delta R/R_0)d\nu]_{max}$ where the denominator is the integrated absorption at saturation coverage.

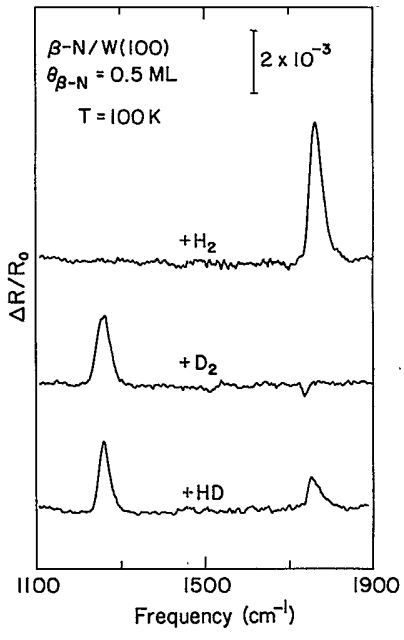

FIG. 6. Change in normalized reflectivity in W—H and W—D-stretch region for H_2, D_2, and HD adsorption onto 900-K-annealed β-N/W(100) at 100 K. Note that for HD the W—D-stretch absorption is larger than the W—H-stretch absorption. The small negative feature for D_2 adsorption is due to displacement of ambiently adsorbed H_2.

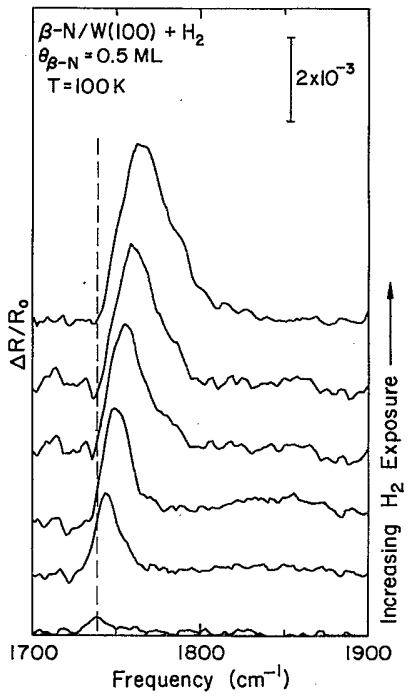

FIG. 7. Change in normalized reflectivity in W—H-stretch region vs H_2 exposure onto $\theta_{\beta\text{-N}}=0.5$, 900-K-annealed β-N/W(100) at 100 K. As the H_2 coverage increases, the center frequency shifts from 1738 to 1766 cm^{-1} while the FWHM increases from 12 to 35 cm^{-1}. Note that the higher coverage lines are more asymmetric than those at lower coverages.

There is a possible problem with just such a coverage determination which needs to be discussed. For dilute impurity systems, such as defects in bulk solid-state materials, integrated absorption strength is a good measure of the relative number of centers participating in the absorption since the small number of molecules does not substantially change the dielectric constant of the host. For a rather highly condensed system of a monolayer or near-monolayer aggregation of absorbers on a metal surface, one must consider the change in the dielectric constant of the layer as the number of centers is increased. More exactly, for a surface density N_s (cm^{-2}) of oscillators with dynamic charge e^* and effective mass μ,

$$\int (\Delta R/R_0) d\nu \propto N_s (e^*/\epsilon_\infty)^2 \mu^{-1} , \quad (1)$$

where ϵ_∞ is, in the three layer macroscopic model of McIntyre and Aspnes[25], the low-frequency part of the electronic response of the overlayer describing the adatoms or admolecules. For example, in the case of the highly polarizable molecular CO species adsorbed on a metal surface, ϵ_∞ can increase from 1 at zero coverage to ~ 2 at a monolayer coverage.[26] For hydrogen adsorption, however, neglect of this term may not be too bad an approximation. For the CO molecule there are many higher-frequency electronic transitions which can contribute to ϵ_∞. In contrast, the electronic simplicity of the H atom is not expected to drastically alter the effective ϵ_∞ of the surface region as the coverage is increased. So with this possible caveat in mind, we proceed with the results.

Figure 8 shows the change in center frequency of the W—H and W—D modes for H_2 and D_2 adsorption, respectively, as a function of on-top coverage. Qualitatively both curves monotonically increase with fractional on-top coverage (θ_f) until a given point, $\theta_f \approx 0.60$ for D and $\theta_f \approx 0.75$ for H, after which the center frequency remains approximately constant. The total shift for H_2 is 28 cm^{-1} while that for D_2 is only 12 cm^{-1}.

The change in peak width is also similar for H_2 and D_2 adsorption onto the 100-K β-N/W(100) surface. As is evident in Fig. 9 the full width at half maximum (FWHM) increases from ~ 12 to 35 cm^{-1} at saturation for both isotopes although the path taken for D is slightly below that of H. Also drawn in the picture is a dotted curve which is $1/\sqrt{2}$ times the solid curve which follows the H data.

Concurrent with the increase in ir absorption is an increase in H_2 thermally desorbed from the W(100) surface. Plotted in Fig. 10 are the areas of the LT-peak, LT-broadband, and HT-peak sections of the TD trace. Both the HT-peak and LT-broadband parts are linear in θ_f while the LT-peak section shows a marked increase in area at $\theta_f \approx 0.7$–0.8.

As noted above, more D_2 sticks to the surface than does H_2. This observation led to the following experiment. First, a saturation exposure (0.7 L) of H_2 was adsorbed on the surface. The change in reflectivity is shown in curve *A* of Fig. 11. (This curve also illustrates the havoc atmospheric water-vapor lines can sometimes cause in even a nominally dry system.) This was followed

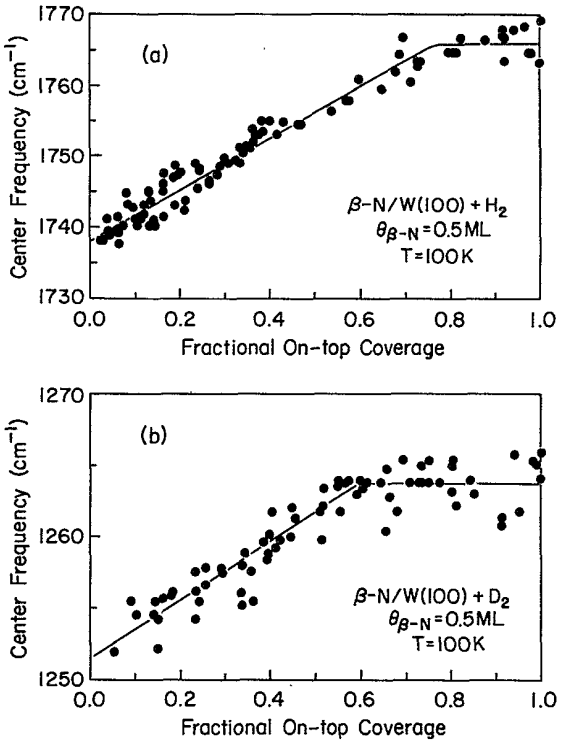

FIG. 8. Center-frequency position vs coverage of on-top H and D for adsorption onto $\theta_{\beta\text{-N}}=0.5$, 900-K-annealed β-N/W(100) at 100 K. The total shift for H coverage is 28 cm^{-1} while that for D is only 12 cm^{-1}. The initial linear regions of the solid curves (before the breaks at 0.6 and 0.75 for D and H, respectively) are least-squares fits to the data below the break. The constant-value portions of the solid curves are drawn as a guide to the eye.

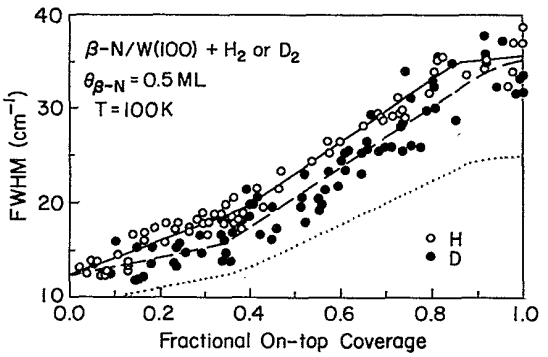

FIG. 9. FWHM of W—H and W—D lines vs on-top coverage for H_2 and D_2 adsorption onto $\theta_{\beta\text{-N}}=0.5$, 900-K-annealed β-N/W(100) at 100 K. As the coverage increases both lines increase in width from 12 to 35 cm^{-1} although the paths are slightly different. The solid (——) and dashed (— — —) lines are guides to the eye for the H and D data, respectively. The dotted curve (· · · ·) is the same as the solid curve divided by $\sqrt{2}$.

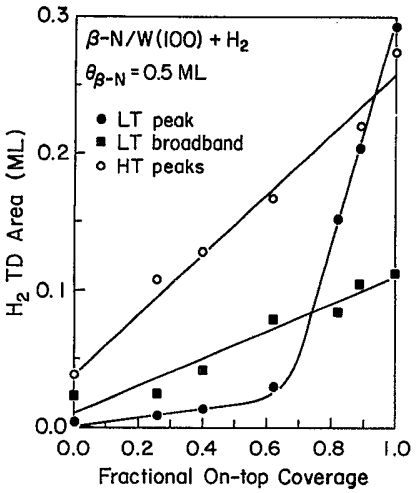

FIG. 10. Amount of H_2 desorbed vs on-top coverage for H_2 adsorption onto $\theta_{\beta\text{-N}}=0.5$, 900-K-annealed β-N/W(100) at 100 K. Both the low-temperature (LT) broadband and high-temperature (HT) portions are linear with coverage while the LT peak turns on strongly at ~0.7 of saturation. Heating rates are 1.4 K sec^{-1} for the LT parts (no *e*-beam current) and 40 K sec^{-1} for the HT peaks (*e*-beam current on). The solid lines are guides to the eye.

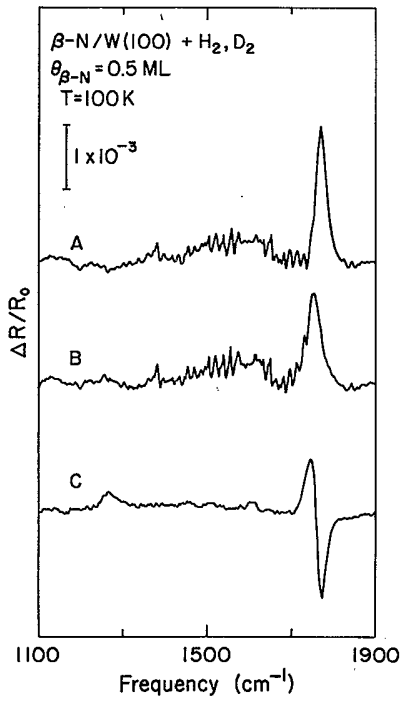

FIG. 11. ir results for saturation H_2 adsorption followed by D_2 adsorption onto $\theta_{\beta\text{-N}}=0.5$, 900-K-annealed β-N/W(100) at 100 K. Curve *A* shows the normalized change in reflectivity (compared to the clean surface) for a saturation exposure of H_2. D_2 adsorption on top of the H_2-saturated surface causes the W—H line to broaden slightly and shift from 1766 to 1755 cm^{-1} as displayed in curve *B*. The difference in curves *A* and *B* (shown in curve *C*) clearly displays the downward shift of the W—H line along with a small W—D line. The noise between the W—H and W—D-stretch regions is due to slight sample drift between the reference spectrum and those after adsorption which causes sharp atmospheric water-vapor lines to be inadequately ratioed to 1.

by an equivalent exposure of D_2. The change in reflectivity normalized to the pure β-N/W surface is shown in curve *B*. Somewhat surprisingly, the W—H line has gotten broader, FWHM≈41 cm^{-1}, and has moved down in frequency to 1755 cm^{-1}. Curve *C* is the difference between curves *A* and *B*. Not only is the W—H shift more clearly shown along with a small decrease in area, but there is a small increase in absorption in the W—D region. In the TD spectra following this sequence, D_2 is desorbed in the γ' peak with the amount (=0.11 ML) equal to the difference in γ' desorption for solitary H_2 and D_2 saturation exposures (see Table II). This observation confirms that the differences in γ' desorption are due to molecularly adsorbed species on the β-N/W(100) surface. In contrast, only ≈0.014 ML is desorbed as D_2 above RT. In the reverse experiment where H_2 exposure follows saturated D_2 exposure, no change in the H-D line and no H_2 TD peaks are observed.

3. *LT annealing experiments*

In hopes of determining the well depth of the on-top site, ir measurements were made as the sample temperature was raised above 100 K after initial exposure. It was found that the ir area remaining at a given temperature is largely insensitive to the rate of temperature change over which ir data could be collected. The next attempt was instead to measure the decay of the ir absorption as a function of time at a given elevated temperature, where upon it was discovered that for a given anneal temperature, the ir area decays to a certain finite value and remains there for as long as the sample remains at that temperature.[27] In addition, cooling the sample back to 100 K effects no increase back towards the initial on-top coverage. Hence, the H atoms are permanently lost to the on-top site once they have been thermally dislodged.

Figure 12 displays, for initial saturation coverage, the percentage of on-top coverage remaining after annealing to temperatures between 100 and 200 K. Results for H and D are essentially identical. Although not shown on the graph, annealing to RT removes all the atoms from the on-top sites.

As a function of initial coverage, the thermal annealing results are also quite interesting. As shown in Fig. 13, for an anneal temperature of 140 K the remaining ir area monotonically increases to ~35% for an initial $\theta_f \approx 0.7$ and then levels off. Also graphed is the ir area which disappears upon annealing. (Both sets of data simply add up to the initial ir area represented by the dashed line.)

TD data taken concurrently with the 140-K anneal ir data are displayed in Fig. 14. H_2 desorbed during the anneal ($\leq$140 K) as well as the remaining H_2 flashed off afterwards (>140 K) are plotted versus initial θ_f. Not unexpectedly, the ≤140-K data are quite similar to the LT-peak data of Fig. 10 while the >140-K data mimic the sum of the LT-broadband and HT-peak results.

In order to check a possible correlation between the ir area gone for a 140-K anneal and the amount of H_2 desorbed below 140 K data of the last two figures are combined in Fig. 15. There is clearly no linear relationship between these two quantities.

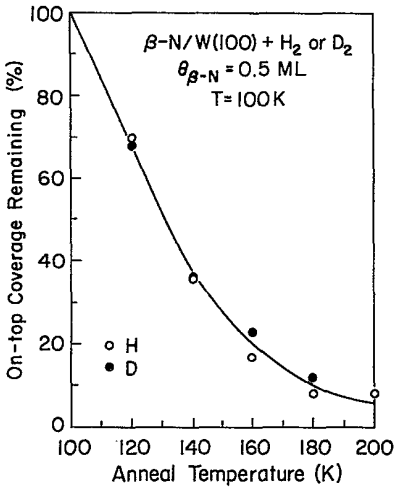

FIG. 12. Effects of anneal temperature on amount of on-top H and D coverage. After H_2- or D_2-saturated adsorption of a $\theta_{\beta\text{-}N}=0.5$, 900 K-annealed β-N/W(100) surface at 100 K, the sample is annealed to a temperature between 100 and 200 K until the ir absorption is no longer changing. The amount of on-top coverage remaining after this treatment is plotted vs the anneal temperature. The solid line is a guide to the eye.

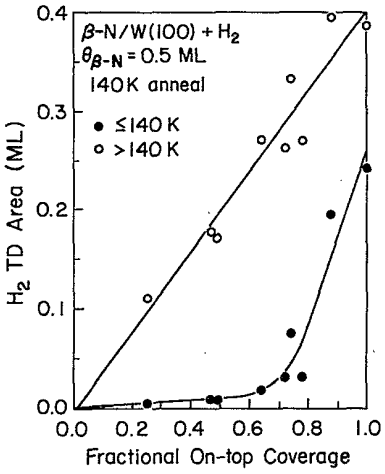

FIG. 14. H_2-thermal-desorption amounts during and after 140-K anneal for various on-top H coverages. After H_2 exposure of a $\theta_{\beta\text{-}N}=0.5$, 900-K-annealed β-N/W(100) surface at 100 K, the sample is annealed to 140 K until the ir absorption is no longer changing. Plotted are the amounts of H_2 thermally desorbed during the 140-K anneal and in a subsequent high-temperature flash.

4. *Isotopic-dilution experiments*

The causes of coverage-dependent frequency shifts, such as those presented in Fig. 8, can be conveniently divided into two categories: (1) chemical shifts and (2) dynamical coupling shifts. Chemical shifts come about from a coverage-dependent chemical environment. It is reasonable to assume, and has been shown, e.g., for several CO-metal-surface chemisorption systems,[28] that nearby adsorbed species can exert a chemical (i.e., static) influence on an adatom's or admolecule's bonding to the substrate and therefore affect its vibrational spectrum. Likewise, dynamical coupling effects occur whenever interactions between the individual oscillators are nonzero. For an ordered overlayer with interactions the proper description is phonons, the ir radiation probes the $q_\parallel \approx 0$ phonon. Going to the isotopically dilute limit from the full-layer situation, assuming there exist no chemical changes, is essentially equivalent to turning off the vibrational interactions within the layer which thereby kills the dispersion-inducing, i.e., dynamical, shifts in frequen-

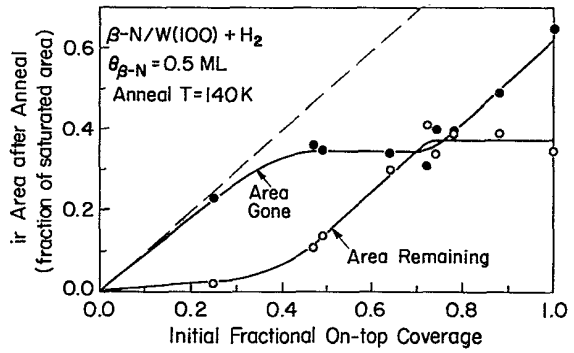

FIG. 13. Effect of 140-K anneal on various coverages of on-top H. After H_2 exposure of a $\theta_{\beta\text{-}N}=0.5$, 900-K-annealed β-N/W(100) surface at 100 K, the sample is annealed to 140 K until the ir absorption is no longer changing. Plotted are the amount of ir area remaining (=on-top coverage remaining) and the amount of ir area gone after the 140-K anneal. The dashed (— — —) line, which is the initial ir area, is the sum of the two solid (——) lines which are drawn as guides to the eye.

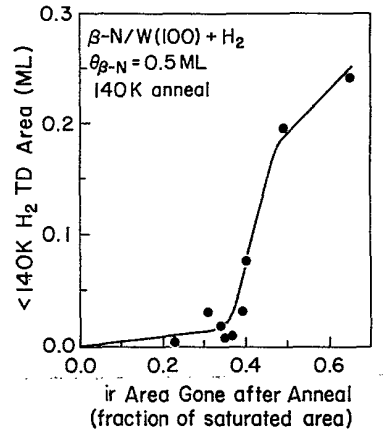

FIG. 15. Amount desorbed vs on-top coverage depletion during 140-K anneal. After H_2 exposure of a $\theta_{\beta\text{-}N}=0.5$, 900-K-annealed β-N/W(100) surface at 100 K, the sample is annealed to 140 K until the ir absorption is no longer changing. Plotted is the amount of H_2 desorbed during the anneal (see Fig. 14) vs the amount of ir area which disappeared because of the anneal (see Fig. 13). A highly nonlinear relationship is shown. The solid curve is drawn as a guide to the eye.

cy. In general both types of shifts occur as the coverage is increased.

Isotopic-dilution experiments can be used to separate out the two kinds of shifts, thereby allowing some measure of the changing chemical environment as well as the dispersion of the high-coverage-limit spectrum. In principle this is done by (1) measuring the frequency ω_0 of a single adatom or admolecule adsorbed on the surface, (2) measuring ω_1, the condensed-layer (saturation coverage in this case) frequency, and (3) measuring ω_2, the frequency of one atom in a condensed layer made up of an isotopic host. The difference $\omega_2-\omega_0$ is then the chemical shift since the isolated atom in the isotopic host is dynamically uncoupled from the host atoms and $\omega_1-\omega_2$ is the dynamical shift since both condensed layers are chemically the same.

In practice things are a bit more difficult since it is impossible to measure the frequency of a single adspecies. Therefore center frequencies are measured as a function of coverage and extrapolated to zero coverage or zero percent dilution. Figure 16 shows the results for isotopic-mixture (H_2, D_2) adsorption onto the β-N/W(100) surface. The isotopic-mixture data are the points with the error bars, and the solid lines are linear least-squares fits to the data. Also illustrated are the frequencies of the W—H and W—D modes for HD adsorption. Previous fits to the coverage-dependent data in Fig. 8 are given by the dashed lines. Preliminary analysis of the data leads to the following identifications: for the W—H mode $\omega_0=1738$ cm^{-1}, $\omega_1=1766$ cm^{-1}, and $\omega_2=1742$ cm^{-1} while for the W—D mode $\omega_0=1252$ cm^{-1}, $\omega_1=1264$ cm^{-1}, and $\omega_2=1261$ cm^{-1}. However, as is delineated more fully in the discussion section, IV D, the identified values of ω_1 and ω_2 are not quite as they were defined above since it is already known that the full H ($+H_2$) layer is not chemically the same as the full D ($+D_2$) layer.

The percentage of H (and therefore D) for the HD and the H_2-D_2 mixtures is determined by the relative ir areas, suitably scaled by the effective mass μ for the mode of the W—H and W—D ir lines. This determination agrees, to within ~2% for all mixtures, with that obtained from a mass spectrometric analysis of the isotopic mixture after the $1/\sqrt{m}$ impingement rate is accounted for. This agreement implies equivalent adsorption rates into the on-top site for both H_2 and D_2 isotopes.

Since the data in Fig. 16 are actually for a 0.7-L exposure of the mixture, which saturates the W-isotope mode but does not necessarily saturate all of the molecular sites, the chemical layer is slightly different for each mixture. This is evident in Fig. 17 which shows a continuous increase in total coverage as the percent D is increased, with the greatest increase coming in the LT-peak part of the TD spectrum. Fortunately, these chemical differences are not a particularly large hindrance to the determination of the dynamic shifts with the layers.

Linewidths of the W—H and W—D absorptions within the isotopic mixtures are presented in Table III. With increasing D percentage both FWHM's increase at an average ratio of 1.25±0.07 for the W—H to W—D width.

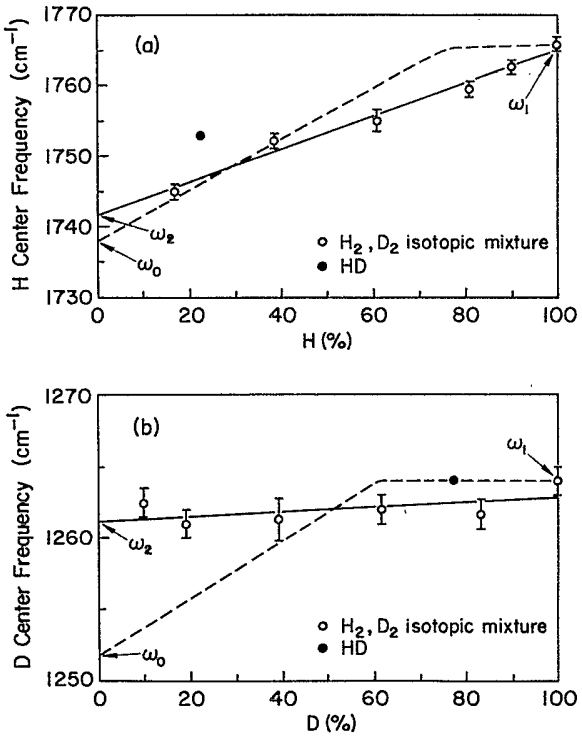

FIG. 16. Isotopic-dilution shifts for H_2-D_2 mixtures onto $\theta_{\beta\text{-N}}=0.5$, 900-K-annealed β-N/W(100) surface at 100 K. ω_0, ω_2, and ω_1 are as defined in the text. Also shown [dashed lines (– – –)] are the fits to the data of Fig. 8.

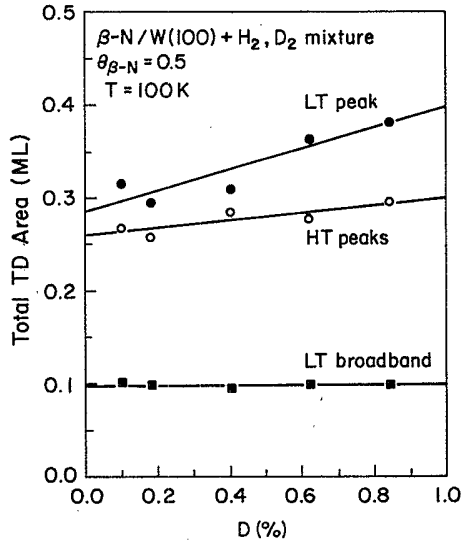

FIG. 17. TD areas during isotopic-dilution measurements. Shown are the amounts desorbed into the LT-peak, LT-broadband, and HT-peak sections of the TD spectra for 0.7 ML exposure of H_2-D_2 mixtures onto a $\theta_{\beta\text{-N}}=0.5$ ML, 900-K-annealed β-N/W(100) surface at 100 K. The solid lines are linear fits to the data.

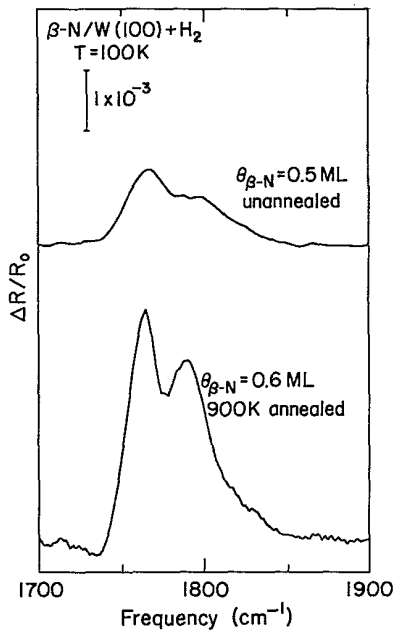

FIG. 18. $\Delta R/R_0$ for H_2 adsorption onto nonstandard β-N/W(100) surfaces. The top trace is for adsorption onto a $\theta_{\beta\text{-N}}=0.5$ ML, unannealed surface at 100 K. The bottom trace is for adsorption onto a $\theta_{\beta\text{-N}}=0.6$ ML, 900-K-annealed surface at 100 K.

D. ir experiments on other β-N/W(100) surfaces

Several other experiments were carried out to further elucidate the nature of N_2 adsorption on the W(100) surface; the results are shown in Fig. 18. The top curve is for saturation H_2 exposure on an unannealed $\theta_{\beta\text{-N}}=0.5$ ML surface and the bottom curve for saturation H_2 exposure on a $\theta_{\beta\text{-N}}=0.6$ ML, 900-K-annealed surface. Each absorption shows both 1766 and 1790 cm^{-1} features implying a similar local environment for the on-top H atoms.

IV. DISCUSSION

A. Assignment of the ir mode

1. Atomic or molecular hydrogen species?

The first question to be answered concerning the ir vibration is whether it is associated with an atomic or molecular species of hydrogen. The results for the HD adsorption, which show two modes (Fig. 6), each within the range of frequencies spanned by the comparable mode for either H_2 or D_2 adsorption, is the strongest evidence available that the species is atomic in nature.

While it is possible that there could exist an accidental degeneracy between molecular H_2 and D_2 modes and two molecular HD modes, the possibility seems marginal. For a perpendicularly oriented molecule the possibility can be fairly easily ruled out. In this case the ir mode has character consisting of mostly either the internal H—H stretch or the W—H_2 stretch. In both cases the two similar HD modes (i.e., WD—H and WH—D or W—DH and W—HD) should not be very different and should both lie between the D_2-induced and H_2-induced frequencies, at $\sim$1530 cm^{-1} for the internal stretch and $\sim$1440 cm^{-1} for the W-molecule stretch. (The internal H—H stretch, which lies at 4159 cm^{-1} for the free molecule, is not expected to lie this low anyway.) For other bonding geometries a myriad of possibilities exists, so an accidental degeneracy is a remote possibility and cannot be completely ruled out. However, for parallel orientation at several high-symmetry sites, Adnot and Carette[29] have shown, for the case of the clean W(100) hydrogen modes, that accidental degeneracy of this type does not occur for reasonable force-constant values.

Also against the molecular-species idea is the integrated areas of the D_2- and H_2-induced modes. After scaling the D_2-induced mode by 2 in order to correct for the ratio of effective masses, the areas of the modes at saturation are 0.171 ± 0.005 cm^{-1} for deuterium and 0.176 ± 0.005 cm^{-1} for hydrogen for the data of Fig. 6.[24] That is, to within errors they are equal. This is in contrast to the thermal-desorption results which suggest that more molecular D_2 is adsorbed than molecular H_2. In fact, the scaled, summed areas for HD equal 0.175 ± 0.005 cm^{-1} which implies, within experimental error, an equal number of atoms participating in the absorption for each isotope.

The magnitude of the absorption also points to an atomic H stretch. Rewritten in terms of microscopic parameters, the right-hand side of Eq. (1) becomes

$$\left[\frac{e^*}{\epsilon_\infty}\right]^2\frac{1}{\mu}=\frac{\alpha_v\omega^2}{(1+\alpha_e U_0)^2} \tag{2}$$

where α_v and α_e are the vibrational and electronic polari-

TABLE III. Linewidths of W—H and W—D stretches for adsorption of isotopic mixtures.

% D (on-top site)	W—D linewidth (cm^{-1})	W—H linewidth (cm^{-1})	W—H/W—D linewidth ratio
0		35±2	
10		34	
19	26	34	1.31
39	30	35	1.16
62	32	39	1.22
83	35	47	1.34
100	35±2		
77[a]	28	34	1.21

[a]HD adsorption.

zabilities, respectively, at the H atom site, and U_0 is the electric field at a given site due to perpendicularly oriented unit dipoles at all other sites. To a first approximation μ, ϵ_∞, and α_v are constant for any perpendicular H vibration on the W(100) surface so that e^*/ϵ_∞ is proportional to the vibrational frequency ω. Scaling the dynamical charge $e^*/\epsilon_\infty = 0.059e$ of bridge-bonded H on the clean W(100) surface[30] by the appropriate frequency ratio (1766 cm^{-1}/1069 cm^{-1}) yields a predicted strength of $e^*/\epsilon_\infty = 0.098e$. As is discussed in Sec. IV E, the maximum coverage of the present ir-active species is 0.67×10^{15} cm^{-2} which yields a measured value of $e^*/\epsilon_\infty \geq 0.12e$ in quite good agreement with the predicted value. So while a molecular species cannot be totally excluded, the evidence surely points to an ir-active atomic entity on the β-N/W(100) surface.

2. *Identification of the atomic adsorption site*

The next question concerns the location of the H atom. On the β-N/W(100) surface there are three high-symmetry sites: (1) the empty fourfold hollow, (2) the β-N-filled fourfold hollow, and (3) the on-top adsorption site shown as *a*, *b*, and *c*, respectively, in Fig. 19. These three sites, which are the only ones to produce a single ir-active mode, are now considered in turn. An idea of the expected frequency for occupation of the empty fourfold hollow can be obtained by comparison with the vibrational frequencies of H on other transition metals in highly coordinated positions. For fourfold adsorption on the fcc Rh(100),[4] Ni(100),[3] and Pd(100) (Ref. 2) surfaces, the H symmetric stretch is located at 665, 630, and 510 cm^{-1}, respectively, for 1 ML coverage. This factor of 3 lower frequency for these three systems does not bode well for a fourfold hollow assignment. Although such a site on a bcc lattice may produce a somewhat higher frequency due to the relatively closer second W layer, the frequency is still expected to be below that for the bridge site[31] which on W(100) has its symmetric stretch at 1069 cm^{-1}.[8] In fact, a recent effective-medium theory (EMT) calculation by Norlander *et al.*[32] predicts a symmetric-stretch frequency of 725 cm^{-1} for the hollow. The highly coordinated fourfold hollow can therefore be ruled out as producing the 1766-cm^{-1} mode.

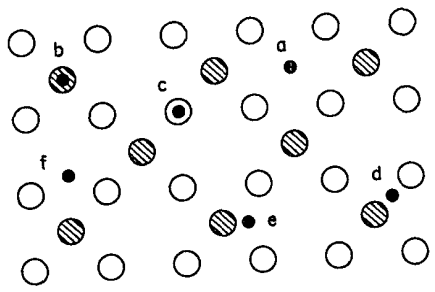

FIG. 19. β-N/W(100) surface depicting possible H-adsorption sites. The open circles are W, shaded circles are N, and the small solid circles are H atoms. The three high-symmetry sites are *a*, the fourfold hollow; *b*, the β-N-filled hollow; and *c*, the on-top W site. Several lower-symmetry sites are also shown; *d*, the W—N bridge; *e* the W_2N asymmetric threefold hollow; and *f*, the distorted-bridge site.

A site not available on the clean W(100) surface is the fourfold β-N-occupied site in which the H atom sits on top of the N atom. The expected frequency can be obtained by comparison with the N—H stretch in simple molecules and with the N—H stretch in *M*—NH_3 complexes where *M* is a metal atom of some sort. In both these cases the frequency is quite high, 3200–3500 cm^{-1} for single molecules and 3000–3400 cm^{-1} for a more highly coordinated N atom in the complexes.[5] In addition, the pioneering EELS work of Propst and Piper detected the presence of an ~3200-cm^{-1} line for activated H adsorbed onto a β-N/W(100) surface which they attributed to the N—H stretch.[33] It thus appears that this site produces a frequency which is too high to explain the observed absorption.

The last high-symmetry site is the on-top site where the H atom is bonded to one W atom. A comparison with *M*—H complexes is encouraging for such an assignment. For these systems the *M*—H-stretch frequencies are observed to be between 1700 and 2250 cm^{-1}.[5] An example with W—H bonds is the cyclopentadienyl complex $(C_5H_5)_2WH_2$ (Ref. 34) which exhibits a W—H stretch of 1922 cm^{-1}, ~10% higher than the presently observed mode. Also in agreement with this assignment are the EMT calculations of Norlander *et al.*[32] which predict a generic on-top *M*—H frequency of 1690 cm^{-1} for transition-metal surfaces.

Before the high-symmetry on-top assignment can be made, there are two other lower-symmetry sites which deserve attention. These are the W—N bridge site and the asymmetric threefold site formed by two W's and one N, also depicted in Fig. 19 as *d* and *e*, respectively. [The site labeled *f*, the distorted bridge away from a β-N atom has been identified in RT EELS data[13] on β-N/W(100)+H_2. It has an ir-active mode at 930 cm^{-1}.] Part of the problem with these sites is that they should each have two ir-active modes. It seems plausible, however, that with higher H coordination the N—H-stretchlike vibration might fall into the 1700-cm^{-1} range and that the vibration which contains more of the metal-substrate–H stretch might be too small to be detected or out of the frequency range of the IRAS experiment.

The best evidence that these lower-symmetry sites are not correct is the observation that the integrated intensity of the vibration is not proportional to the β-N coverage. For these two sites a reasonable assumption about their existence is that only one β-N atom is needed per site so that β-N coverage should be proportional to ir-active H coverage. In contrast, for the on-top position the simplest assumption that can be made for its viability is that two nearest-neighbor β-N atoms (which are collinear with the W atom) are needed to produce barriers large enough to keep the H atom out of one of the four neighboring bridge sites. From this it follows if all possible sites are occupied, as depicted in Fig. 20, then at the lowest coverages $\theta_f/\theta_{\beta\text{-N}} = 0.5$ and at $\theta_{\beta\text{-N}} = 0.5$ ML, $\theta_f/\theta_{\beta\text{-N}} = 2.0$, so that there is a faster than linear change in θ_f with β-N coverage.

As can be discerned from Fig. 2 and is discussed in more detail in the next section, there is a faster than proportional dropoff in $\int(R/R_0)d\nu$ versus β-N coverage as the β-N coverage is reduced from $\theta_{\beta\text{-N}}=0.5$. While not expected for these two low-symmetry sites (and also the fourfold β-N-filled site), *this behavior is exactly as expected for the on-top site.* While also reserving the detailed discussion until the next section, the on-top site also explains the leveling off of $\int(R/R_0)d\nu$ plus the appearance of a second line for coverages of β-nitrogen greater than 0.5 ML. Identification of the vibration thus falls on the W—H stretch for H sitting on top of one W atom situated between two nearest-neighbor β-N adatoms.

B. H as a probe of the β-N layer

LEED studies have shown that β-nitrogen tends to form islands at all coverages.[11] Qualitatively this is also evident in Fig. 1 which shows a constant center frequency versus $\theta_{\beta\text{-N}}$ at saturation. A constant center frequency is expected (and has been observed[35]) for island formation since on a local scale (a few lattice sites) the layer is the same as a complete overlayer for most of the adlayer.

A bit more information on the β-N islands can be gleaned from the ir data. As depicted in Fig. 20, the $\theta_f/\theta_{\beta\text{-N}}$ ratio is sensitive to the size of the β-N islands.

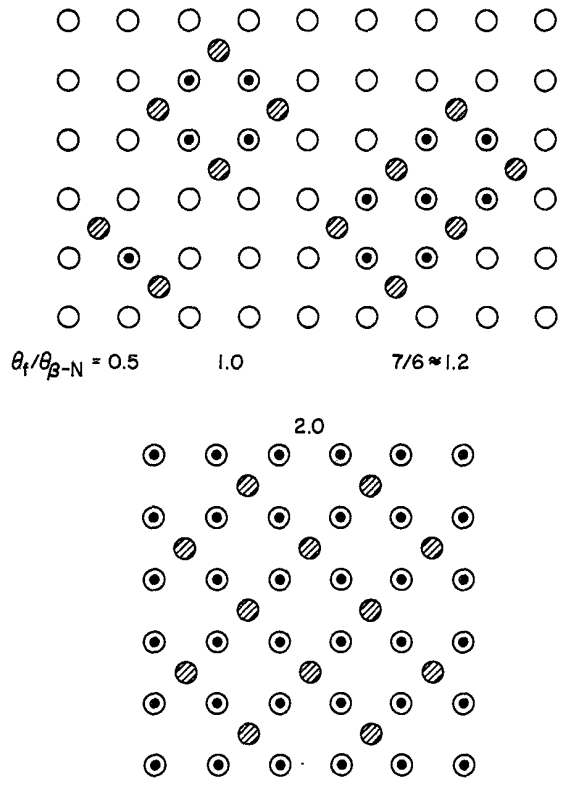

FIG. 20. Idealized model of H adsorption onto β-N/W(100). The open circles are W, shaded circles are N, and the small solid circles are H atoms. As $\theta_{\beta\text{-N}}$ increases, the ratio of θ_f to $\theta_{\beta\text{-N}}$ increases from 0.5 for a β-N island of two to 2 for $\theta_{\beta\text{-N}}=0.5$ ML.

Small islands support relatively fewer on-top H's than do large islands. Hence, the absorption strength of the W—H vibration should be some measure of the average β-N island size for a particular β-N coverage.

While this nonlinear relationship can be discerned from Fig. 2, the data can be plotted in a more transparent form as shown in Fig. 21 where N_2 exposure has been converted to $\theta_{\beta\text{-N}}$ and $\int(R/R_0)d\nu$ has been converted to θ_f where in this figure it is assumed that $\theta_f/\theta_{\beta\text{-N}}=2$ at $\theta_{\beta\text{-N}}=0.5$. As expected the ratio $\theta_f/\theta_{\beta\text{-N}}$ decreases as $\theta_{\beta\text{-N}}$ decreases. (As discussed in the last section, for the two lower-symmetry and on-top β-N sites a constant value is expected.) It is interesting that at intermediate β-N coverage a plateau is evident. This implies that there exists a preferential β-N island size, which is perhaps not surprising. One LEED study done at $\theta_{\beta\text{-N}}=0.4$ (Ref. 12) suggests that an island size of 16 is highly stabilized by a β-N-induced reconstruction of the top-layer W atoms. The ir data indicate that this structure is possibly stable down to $\theta_{\beta\text{-N}}\approx0.2$, although this is slightly at odds with LEED observations (Table I) which show rather fuzzy half-order beams up to 0.2 L exposure which corresponds to $\theta_{\beta\text{-N}}\approx0.28$. However, given the errors in the ir measurements (Fig. 21), the qualitative correlation between the two techniques is quite good.

Quantitatively, an island size of 16 should result in a $\theta_f/\theta_{\beta\text{-N}}$ ratio of ~1.5.[36] In fact, simple site counting shows that as the β-N size is reduced from 0.5 to 0.4 ML the $\theta_f/\theta_{\beta\text{-N}}$ ratio should, at least approximately, follow the dashed line in Fig. 21. (Initially, e.g., removal of each N results in the loss of four possibly active on-top W sites.) Experimentally, the fall-off is slightly faster than expected. Possibly this is caused by elongated islands although the LEED-deduced reconstruction model does not favor such an interpretation. A likely explanation is that not quite all of the island edge sites are filled due to

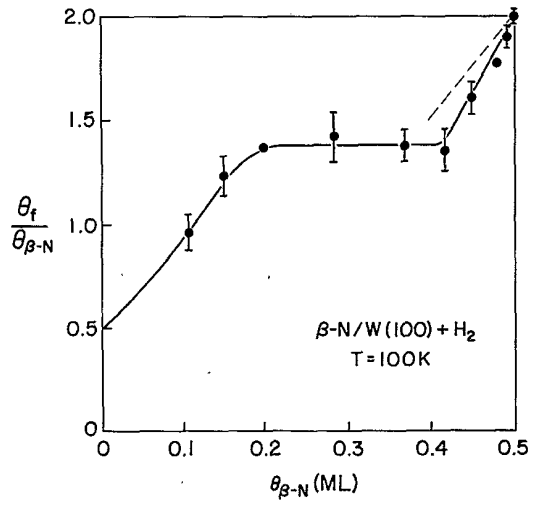

FIG. 21. $\theta_f/\theta_{\beta\text{-N}}$ vs $\theta_{\beta\text{-N}}$. Assuming $\theta_f=1$ ML at $\theta_{\beta\text{-N}}=0.5$ ML, their ratio is plotted as a function of $\theta_{\beta\text{-N}}$. As $\theta_{\beta\text{-N}}$ decreases the ratio sharply drops, levels off at intermediate coverages, and falls again as $\theta_{\beta\text{-N}}\rightarrow0$.

interaction with H adsorbed on the clean-W part of the surface. At $\theta_{\beta\text{-N}}=0.4$, assuming 4×4 islands, the data imply that if all the on-top sites are filled at β-N saturation then ten of a possible 12 on-top edge sites are filled at this lower coverage; hence, this effect is not particularly large.

As demonstrated in Figs. 1 and 18, H adsorption on a β-N surface can lead to a line at 1790 cm^{-1} as well as the 1766-cm^{-1} feature. Since the integrated intensity versus $\theta_{\beta\text{-N}}$ is essentially constant for $\theta_{\beta\text{-N}} \geq 0.5$ ML, it appears that the total number of active sites is not changed for greater than 0.5 ML β-N coverage (this is also consistent with the on-top W assignment). However, at these coverages the N atoms no longer have the luxury of sitting on a $c(2\times2)$ lattice: some must fill sites next to other β-N atoms. This produces surface W atoms which have three nearest-neighbor β-N atoms. It is not surprising, therefore, that a new line appears at 1790 cm^{-1} under these crowded conditions.

Neither is it surprising that such crowded conditions occur on the unannealed β-N surface. As is evident in LEED observations, sharp $c(2\times2)$ spots occur only with above-RT annealing. It is interesting that the $\theta_{\beta\text{-N}}=0.5$ ML unannealed surface produces a much weaker absorption than the 0.6 ML annealed surface and suggests two possibilities: (1) there are other sites besides the fourfold hollow sites which become nitrogen filled without annealing which block on-top adsorption; (2) fourfold sites are still only filled but that four nearest-neighbor β-nitrogens are sufficient to quench on-top H adsorption. This last possibility seems more likely since EELS (Ref. 13) has identified only one RT adsorption site.

C. Linewidth

Linewidth measurements are intrinsically appealing since there always lurks the possibility of extracting dynamical information—a lifetime or a dephasing time—from a relatively simply obtained quantity. For H on clean W(100), H interactions appear to substantially contribute to the symmetric stretch width,[8] while electronic damping seems to control the wag-overtone line shape.[37] In the present case of the W—H stretch it is seen that electronic damping may play a role at low coverage, but inhomogeneous broadening apparently dominates at higher coverages.

1. Zero-coverage limit—electron-hole pair decay?

The best route, with linear spectroscopy, to identification of an underlying physical process is utilization of temperature- and isotope-dependent studies in conjunction with some sort of detailed theoretical calculation. In the present system T-dependent measurements are ruled out simply because the adatom site is not constantly populated as the temperature is raised. However, several calculations[38] on the electronic damping of H do invite comparison with the zero-coverage-limit FWHM minimum of 12 cm^{-1} for the W—H and W—D modes. In this limit inhomogeneous broadening should be at a minimum because it appears that there are fewer other states, such as molecular H_2 or D_2, to interfere with the on-top adatoms.

The calculations predict, in the absence of any special resonance near the Fermi level (a weak breakdown of adiabaticity), that the H atom's perpendicular vibration is damped by the free carriers of the metal with a rate which depends upon the local density of carriers. For W a FWHM $\approx$ 15 cm^{-1} is calculated which compares favorably with the measured value of 12 cm^{-1} (Fig. 9). The problem with this electron-hole pair generation mechanism is the expected isotope dependence to the linewidth. A $1/\mu$ dependence predicts a W—D linewidth which is half that of the W—H line.

Although W is certainly not free-electron-like on a detailed level, it is unknown whether this can account for the apparent isotopic independence of the zero-coverage-limit width within the framework of electronic damping. A recent calculation of electron-hole pair damping in the limit of a strong breakdown of adiabaticity predicts a $(1/\mu)^{1/2}$ isotopic dependence to the linewidth[39] which suggests that the W—D width should be 8.5 cm^{-1} given the W—H width of 12 cm^{-1}. Experimentally, however, the W_2H wag overtone on W(100), which has been shown to decay via electronic excitations in the strong-breakdown limit, has linewidths for the W_2D and W_2H vibrations of 25 and 22 cm^{-1}, respectively;[30] i.e., the D mode appears even a bit broader than the H mode. Clearly, detailed information on the surface electronic structure of β-N/W(100)+H_2 is needed in order to resolve this question of electron-hole pair coupling and decay.

2. Higher coverages—inhomogeneous broadening

The simplest expectation for the isotopic dependence of a disorder-broadened FWHM is $1/\sqrt{\mu}$. This comes, in a ball and spring model, from the assumption of an identical distribution of spring constants independent of the isotopic mass. First consideration of the θ_f-dependent FWHM for H and D in Fig. 9 suggests that something else besides inhomogeneous broadening is dominating the linewidth. The figure shows that the D width is only slightly less than the H width at all coverages except zero and saturation where they are equal. The dotted line is the same as the H-fitted solid line except it is scaled by the factor $(\mu_H/\mu_D)^{1/2}=0.707$. Clearly it does not match the W—D linewidth.

This comparison of linewidths is not completely valid. It has already been shown that the saturated-D and saturated-H surfaces are not chemically the same—i.e., more molecular D_2 than H_2 is adsorbed on its respective surface. It is certainly reasonable to assume that the same is true at lower coverages which suggests that molecular H_2 (or D_2) is responsible for some part of the linewidth.

The isotopic-dilution data for saturation θ_f compiled in Table III support this notion. As the D percentage increases, it is clear that both linewidths increase. This increase in FWHM with greater D percentage is accompanied by an increase in the total (most likely molecular) coverage which is shown in the TD areas of Fig. 17. Figure 11 also directly shows the same increase in W—H

FWHM from 33 to 41 cm^{-1} when D_2 is adsorbed on top of the already H-saturated β-N surface. Therefore it is most likely that the D-coverage widths of Fig. 9 are slightly pushed up due to extra adsorbates not present on the equivalent on-top H-coverage data.

The isotopic-dilution data also provide a more valid comparison of the W—D and W—H linewidths since the chemical environment is identical for the two oscillators within the layer. Table III shows for all mixtures that the W—H FWHM is always greater than the W—D FWHM. The ratio is approximately constant with an average of 1.25 ± 0.07, slightly less than the expected 1.41 due to disorder-induced broadening. It is certainly hard to argue that inhomogeneous broadening does not have an effect here, in light of the correlation with the molecular-species coverage. The numbers do suggest, though, that some other mechanism may also be important in the linewidth determination.

D. Frequency shifts

Figure 16, which shows the frequency shifts for the isotopic mixtures as well as for the production of a full layer from a low-coverage one, hints that there are several underlying frequency-shifting mechanisms. As is evident in what follows, there are two types of chemical shifts present and possibly two types of interactions responsible for the dynamical shifts.

Consideration of the linewidths in the last section showed that the presence of the molecular species can have a definite effect upon the on-top vibration. Hence a more refined identification of ω_0, ω_1, and ω_2 is needed than was presented in the results section. Table IV tabulates values of these frequencies for layers which are chemically identical (except for $\omega_{1,?}$ as discussed below) for H_2 and D_2 chemisorption. As can be seen, there are now two values of ω_2 and three values for ω_1 which are labeled with an extra subscript denoting the state of molecular adsorption.

The H_2 subscript is for a layer which has a saturation amount of molecular H_2. For the W—D mode ω_{2,H_2} is taken to be the ω_2-marked intercept in (b) of Fig. 16. The frequency ω_{1,H_2} is not available for D_2 adsorption since a saturated W—D mode cannot be produced with only a molecular-H_2 saturation amount. For the W—H mode ω_{1,H_2} is the marked intercept in (a) of the figure and ω_{2,H_2} is unavailable since this layer is mostly D_2 and is thus molecular-D_2 saturated.

Likewise, the D_2 subscript is for a layer which has a saturation amount of molecular D_2. For the W—H mode ω_{2,D_2} is the marked intercept in (a) of Fig. 16. The W—H frequency ω_{1,D_2} is deduced from the experiment when a saturated H_2 layer is further exposed to D_2 (see Fig. 11).[40] For the W—D mode ω_{1,D_2} is just the D_2-saturated-layer frequency. The frequency ω_{2,D_2} is also denoted (in parentheses) for the D_2 layer. It is not directly measured but is obtained by adding 3 $cm^{-1}=(1/\sqrt{2})(\omega_{2,D_2}-\omega_0)$ from the W—H column to ω_0 for the W—D mode. It is used later to compare dynamic shifts of the two isotopic absorptions.

There is one other ω_1 frequency, marked $\omega_{1,?}$, in the table. This is obtained by extrapolating the straight-line regions of the dashed lines in Fig. 16 to 100% coverage. The question mark indicates that the molecular composition is really unknown for the two hypothetical layers, but, as suggested by the linewidth analysis, there is probably more molecular D_2 on the D layer than H_2 on the H layer.

This claim is verified by comparing the differences between $\omega_{1,?}$ and ω_0 for H and D. The ratio (37 cm^{-1})/(20 cm^{-1})$=1.85$ is not equal to $\sqrt{2}=1.41$ as expected for chemically identical layers. This is again consistent with relatively more molecular species present on the D_2 exposed surface for equivalent on-top coverages since it is known that the molecular species depresses the on-top frequency. The earlier break in the dashed line for W—D compared to W—H is likely indicative of the earlier presence of molecular D_2 species compared to H_2.

The positions of the W—H and W—D lines for HD absorption can also be understood in terms of the molecular-species suppression of the vibrational frequency. Both of the vibrations are higher than their equivalent W—H and W—D isotopic-dilution counterparts since the isotopic H_2-D_2 mixtures at ~77% D have more adsorbed molecular species than does the HD produced layer.

TABLE IV. W—H and W—D symmetric-stretch frequencies: ω_0 is the zero-coverage frequency, ω_2 is the dilute-isotopic-limit frequency, ω_1 is the saturation-layer frequency. H_2 and D_2 represent saturation amounts of coadsorbed H_2 and D_2 molecular species, respectively. The question mark symbolizes unknown amount of coadsorbed molecular species.

Frequency label	W—H frequency (cm^{-1})	W—D frequency (cm^{-1})
ω_0	1738	1252
ω_{2,D_2}	1742	(1255)
ω_{2,H_2}		1261
ω_{1,D_2}	(1758)	1264
ω_{1,H_2}	1766	
$\omega_{1,?}$	1775	1272

1. Dynamical shifts

The magnitude of the dynamical shift is now easily obtained from $\omega_{1,D_2}-\omega_{2,D_2}$. For W—H the shift is +16 cm^{-1} and for W—D it is +9 cm^{-1}. A weighted average $[(16+9\sqrt{2})/2]$ produces a value of +14 cm^{-1} for the W—H strength. For chemisorption systems two coupling mechanisms have been shown to be important in determining these shifts. For the CO internal stretch, through-space dipole-dipole coupling is apparently the dominant mechanism,[26] while studies of other H systems[2–4] have concluded that an indirect interaction, mediated by the metal electrons, is needed to explain the relatively large shift of the fairly weak M_x-H oscillator. Other coupling mechanisms, such as indirect phonon-

mediated coupling[2] and direct overlap of H wave functions are not expected to be important due to the relatively small H-atom mass and size, respectively.

The dipole-dipole interaction is first considered. For a lattice of perpendicularly oriented point dipoles above a metal surface the absorption strength $\int(\Delta R/R_0)d\nu$ is related to the expected shift $(\nu_1-\nu_2)$ due to vibrational coupling via the equation

$$\int \frac{\Delta R}{R_0}d\nu = 8\pi^2 \frac{4\pi N_1}{U_0}\frac{\sin^2\theta}{\cos\theta}\frac{1}{1+\alpha_e U_0}\nu_2(\nu_1-\nu_2) \tag{3}$$

where $\theta=84°$ is the incident-light angle to the surface normal, $\nu_2=1742$ cm^{-1} is the isotopically dilute center frequency, $N_1=10^{15}$ cm^{-2} is the areal density of adsorption sites, and α_e and U_0 are as defined above.

In order to calculate a frequency shift from Eq. (2) values for the two parameters α_e and U_0 must be obtained. No electronic screening of the W—H mode would result in $\alpha_e=0$. However, for the Pd(100)—H symmetric stretch,[2] it has been estimated that $\alpha_e\approx 1.5$ Å^3 for the fourfold hollow site. Although α_e may be somewhat different for the W(100) on-top site, it seems like a reasonable estimate for the case at hand.

The lattice sum U_0 has two contributions. The first, U_0', equal to the sum of direct fields from the other dipoles, is calculated to be 0.29 Å^{-3}.[41] Image dipoles also contribute a term, U_i, to the electric field at each site. The value of U_i lies between 0 and U_0'; its value is determined by the height D of the oscillators above the effective image plane of the metal surface. In the present case the image plane is estimated to be $\sim$1.05 Å above the top-layer W-atom position[42] and the W—H bond length to be 1.65 Å (Ref. 43) so that $D=0.6$ Å. This yields a value for $U_i\approx 0.15$ Å^{-3} so that $U_0=U_0'+U_i\approx 0.44$ Å^{-3}. The expected shift, taking $\int(\Delta R/R_0)d\nu=0.165$ cm^{-1}, due to dipole-dipole coupling is thus estimated from Eq. (3) to be 7 cm^{-1}, which accounts for only $\frac{1}{2}$ the measured value of 14 cm^{-1}.

The expected shift due to an electron-mediated interaction, which has been invoked to account for dynamical shifts of 27 cm^{-1} on Pd(100),[2] 40 cm^{-1} on Rh(100),[4] and 48 cm^{-1} on Ni(100) (Ref. 3) for the H symmetric stretch is more difficult to estimate since even rather fullblown EMT calculations can only give order-of-magnitude estimations in some cases [72 cm^{-1} compared with 48 cm^{-1} for Ni(100)] for the expected shifts.[44] For the present case an estimation is made based on a consideration of the interaction between two protons on a jellium surface and the H experimental data on these three other surfaces.[45]

The interaction between two protons sitting on a jellium surface has been the subject of several investigations.[46] In general, the interaction potential $\Phi(r)$ behaves approximately as

$$\Phi(r)\approx A\frac{1}{r^5}\cos(2k_F r+\phi) \tag{4}$$

for distances r between the protons such that $2k_F r\gg 1$, where k_F is the Fermi wave vector, ϕ is a phase factor, and A is a constant. Both A and ϕ can depend upon the distance the two protons are from the surface and seem to be rather sensitive to the exact details of the model being considered. Clearly the interaction falls off rapidly but it is also highly oscillatory. However, it has been pointed out by Norlander and Holstrom[44] that for distances corresponding to $p(1\times 1)$ adsorption on Ni(100), Rh(100), and Pd(100) in the fourfold hollow sites (the adlattice constants are 2.49, 2.69, and 2.75 Å, respectively) that the induced charge density due to one adatom at the nearest-neighbor sites is negative and that at other sites (where the oscillations matter) the interaction strength has become negligible. Norlander and co-workers[32,44] further point out that for transition metals the electron-density falloff into the vacuum is well described by a jellium model with $r_s/a_0=2.5$ where r_s is a radius which is related to the electronic density n by $n^{-1}=\frac{4}{3}\pi r_s^3$ and to the Fermi wave vector by $k_F=1.92/r_s$;[47] a_0 is the Bohr radius.

It therefore seems plausible that the dynamical shift for on-top adsorption on W can at least be estimated by fitting the measured shifts for these other three transition metals to a power law in the interadsorbate spacing. Doing so results in the expression $\Delta\nu=3.96\times 10^3 r^{-4.8}$ cm^{-1} where $[r]=$Å. Applying this to $r=3.16$ Å, which is the on-top W spacing, yields $\Delta\nu=+16$ cm^{-1}. This is surprisingly close to the measured dynamic shift of $+14$ cm^{-1}. While there are certainly problems in comparing the results of Ni, Rh, and Pd with W, such as the fact that the H adsorption site is different on W and the fact that W has much smaller valence d-band filling than these other transition metals which tends to invalidate the use of jellium-model response,[32,44] it is clear that obtaining a better estimation of the expected shift would involve a rather detailed theoretical calculation.

One last point should be made about the expected dynamical shifts. As is shown by Schlesinger *et al.*,[48] and is apparent in the work of Persson and Ryberg,[26] shifts due to dipole-dipole coupling are reduced if the inhomogeneous broadening is of the same order as the expected frequency shift $\nu_1-\nu_2$ of the homogeneous line. This is basically because the different oscillators do not want to oscillate at quite the same frequency and therefore do not "lock in" to the frequency ν_1 quite as easily. Such behavior is therefore not expected to be dynamical-interaction dependent and hence should occur for the electron-mediated coupling also. The combined expected shift for a homogeneous mode is approximately $7+16=23$ cm^{-1} while the linewidth analysis suggests that the inhomogeneous broadening is roughly the same size. Therefore the total expected shift for W—H should be reduced somewhat.

In summary, a combination of the through-space dipole-dipole interaction and the indirect metal-electron-mediated interaction can account for the measured dynamical shift of 14 cm^{-1} with perhaps the electron-mediated shift contributing approximately twice as much as the dipole shift. This is in contrast to other M_x—H chemisorption systems where the dipole shift is negligible, but is not surprising given the lower W(100) ML-coverage density combined with the relatively large effective charge $e^*/\epsilon_\infty\approx 0.1e$ compared to, for example,

$e^*/\epsilon_\infty \approx 0.06e$ for bridge-bonded H on W(100) (Ref. 30) or $e^*/\epsilon_\infty \approx 0.02e$ for the symmetric stretch in the four-fold hollow on Rh(100).[4]

2. Chemical shifts

The most obvious chemical shift is that induced by molecular adsorption. There are four experimental facts which clearly demonstrate that molecular coadsorption depresses the frequency of the W—H stretch which we now reiterate. (1) By increasing the molecular coverage from a saturated H_2 amount to a saturated D_2 amount, the center frequency decreases from $\omega_{1,H_2}=1766$ cm^{-1} to $\omega_{1,D_2}=1758$ cm^{-1}, a shift of -8 cm^{-1} (this is essentially demonstrated in Fig. 11). (2) In Fig. 16 the frequency ω_2 for W—H is relatively closer compared to ω_0 than is ω_2 to ω_0 for the W—D mode. (3) The coverage versus frequency curves show a slower initial slope and overall smaller excursion for D_2 compared to H_2 even after the $(\mu_H/\mu_D)^{1/2}=0.707$ factor is taken into account. (4) Compared to the isotopic mixture which produces the same relative coverage of on-top H and D, HD adsorption results in higher vibrational frequencies for both isotopes.

A quantitative estimation of this chemical shift due to molecular coadsorption can be obtained from Table IV. A comparison of $\omega_{1,?}=1775$ cm^{-1}, which is clearly the best choice for a zero molecular coverage ω_1 frequency, and $\omega_{1,D_2}=1758$ cm^{-1} indicates that the total chemical shift due to molecular coadsorption is at least -17 cm^{-1}.

The magnitude of this shift is consistent with the γ' TD results presented in Table II. As discussed above, the HD data imply that the γ' peak is half molecular and half atomic. If it is assumed that the atomic-half amount is isotope independent (this is suggested by the ir annealing data which is discussed in Sec. IV E), then the molecular-species ratio of H_2 to D_2 on the respectively saturated surfaces is 1 to 2.5 so that the total molecular shift is $2.5/1.5=1.67$ times the saturated molecular H_2 to saturated molecular D_2 shift of -8 cm^{-1}. That is, the TD predicted molecular shift is -13 cm^{-1}, in good accord with the -17-cm^{-1} shift from $\omega_{1,?}$ to ω_{1,D_2} for W—H.

There is one other chemical shift which can be identified. The difference in ω_{2,D_2} and ω_0 shows that this shift is $+4$ cm^{-1} greater than the magnitude of the molecular-species-induced shift of -17 cm^{-1}, so this second shift is $+21$ cm^{-1} in going from the isolated adatom to the full layer.

In addition to the electron-mediated dynamical shifts, EMT calculations[44] also predict a chemical shift due to the static change in charge density induced at other sites by the presence of an ad-H. Physically, an adsorbed H atom attracts charge from nearby sites in a manner which induces a larger charge-density gradient normal to the surface at the surrounding sites. The bigger charge-density gradient results in a higher frequency for perpendicular H modes.[49] Hence the chemical shift is positive. (This mechanism also produces the dynamical shift since an H atom farther away from the surface is less well screened and therefore attracts more charge from its surroundings so that an even harder potential is felt for two nearby atoms oscillating in phase.) In the harmonic approximation the static shift is equal to the dynamic shift[44] so, given the estimation in the last section, a shift of $\sim+16$ cm^{-1} is expected in the present case from the presence of all the on-top atoms, which, given the electron-mediated-shift estimation method, is in reasonable agreement with the $+21$-cm^{-1} measured shift.

However, there are, it seems, more atomic species on the surface than just the on-top atoms. This is apparent in the ir results for HD adsorption shown in Fig. 6. The ratio of W—D to W—H absorption strengths implies that there exist 4.4 times as many on-top D's as H's. (It also implies some possibly interesting dynamical effects in the adsorption process.) Since Table II shows that there exist equal amounts of H and D atoms on an HD exposed surface, there must, therefore, be some other atomic species on the surface with a coverage of at least 80% of the on-top site, possibly in the distorted-bridge site f of Fig. 19 which RT EELS measurements of β-N/W(100)+H indicate as a likely binding position. Such adatoms, which are dynamically uncoupled due to their incongruent vibrational spectrum, should still exert a static influence comparable to the on-top atoms and thus perhaps provide some of the positive chemical shift deduced from the data. This ω-changing mechanism also accounts for the higher observed frequency at 1790 cm^{-1} for 3-β-N-atom coordination compared to 1766 cm^{-1} since the atomic N atoms also tend to steal charge from their local neighborhood.

In light of this positive chemical-shift mechanism, the negative chemical shift of molecular adsorption can perhaps be rationalized. Since H_2 is essentially a closed-shell unit, it is perhaps reasonable to expect that it is electropositive; i.e., upon chemisorption it donates some charge to the surrounding sites which therefore largely cancels the positive chemical shift caused by atomic chemisorption.

E. Surface potentials for the hydrogen adlayer

It seems that no single TD feature can be associated with direct desorption of H_2 from the on-top sites. The data of Fig. 12, which show that a constant barrier height cannot be associated with the on-top H as the temperature is raised and the state is depopulated, indicate that any on-top H which does directly come off below RT does so in a broadband fashion. One could therefore try to associate the LT-broadband part of the TD spectrum with on-top H. There is, however, only ~ 0.1 ML of adsorbed H_2 in the LT-broadband part of the spectrum. This amount could be approximately doubled if some of the LT-peak area is included (see Fig. 5) which would then give a saturation coverage of 0.4 ML of on-top H. Such coverage implies that $e^*/\epsilon_\infty=0.16e$ which, by itself, is probably not unreasonable.

However, consideration of the HD exposure result, which exhibits much more on-top D than on-top H and therefore implies the existence of other viable atomic-H sites for 100-K adsorption, intimates that upon warming

the sample some of the on-top H most likely migrates to other sites. That such migration occurs at less than saturation exposure is evident from the 140-K-anneal experiments. As shown in Fig. 15, upon heating to 140 K, an amount of on-top H up to ~40% of saturation can disappear with very little (~0.04 ML H) concurrent thermal desorption.

Although the low-temperature annealing data of Fig. 12 can be rationalized by a wide distribution of parallel-motion potential barriers, the migration of on-top H to other sites can explain the annealing results. Most likely the increasing levels of H at other sites causes the potential well for motion along the surface from the still occupied on-top sites to become effectively deeper. It is interesting to note that this large change in parallel barriers along the surface is *not* accompanied by a substantial change in the perpendicular potential as evidenced by the essential constancy (1754–1768 cm^{-1}) of the W—H symmetric-stretch frequency upon annealing.

For higher coverages, above ~70% of on-top saturation, Figs. 13 and 14 suggest that some on-top H is possibly desorbed during a 140-K anneal. This is due to the correlation of the upswing of ir area gone in Fig. 13 with the upswing of H_2 desorbed during the anneal as displayed in Fig. 14. If half of the TD upswing is attributed to the upswing in ir area gone (remember approximately half the LT peak is from molecular H_2) then ~25% of the saturation ir area corresponds to ~0.25 ML of atomic H which implies ~1 ML of ir-active H for saturation exposure. While this possibility is consistent with the on-top assignment, further consideration of the HD ir absorption strengths (4.4 on-top D's for each on-top H) along with the HD TD data (Table II) reveals that the maximum on-top coverage is only 0.67 ML. Therefore not all of the atomic upswing in TD area can be attributed to ir-active H.

Eventually all the H must come off the sample as it is heated. Above RT there are two distinct β-N-induced H_2 features as shown in Fig. 3. The close proximity of the β_1' feature to the β_1 feature, which is from bridge-bonded H on the unreconstructed clean-W surface, suggests that the β_1' peak is due to TD from a distorted-bridge site such as the one labeled *f* in Fig. 19. As mentioned earlier, EELS has detected a vibrational mode indicative of such a chemisorption location.[13]

Perhaps the most intriguing H_2-TD feature is the β_2' feature which starts out at ~730 K for lower β-N coverages and moves down slightly as $\theta_{\beta\text{-N}}$ approaches 0.5 ML. There are two possible binding sites which come to mind regarding this feature. The first is the on-top β-N site. As mentioned before, the pioneering EELS data of Propst and Piper[33] showed that activated H_2 adsorption on a β-N/W(100) surface results in a 3200-cm^{-1} line attributable to an N—H stretch. Possibly heating the sample during the TD results in some H bonding to the N which later desorbs. The second possibility is that the β-N has somehow allowed the H to go subsurface so that it is bonded to the second layer of W atoms which then results in a higher than clean-surface binding energy. Further investigation, especially of the first possibility, is warranted since the N—H mode should be detectable with the present IRAS setup.

Lastly, we comment upon the unexpected ratio of W—D to W—H ir absorption strengths for HD adsorption. The possibility that this is a kinetic effect caused by D's displacing already bonded on-top H's is largely ruled out by the isotopic-dilution results which exhibit the expected ir-strength ratios for all five mixtures. This seems to indicate that the HD molecule, at the moment it dissociates, is more likely to leave a D atom at the on-top site rather than an H atom. This last possibility seems worthy of future investigation.

V. SUMMARY AND CONCLUSIONS

Investigation of the β-N/W(100) surface upon the adsorption of H_2 with thermal desorption and infrared spectroscopies has revealed a variety of H adsorption states. This chemisorption variety is somewhat surprising given the rather simple bonding on clean W(100) where the H is bridge bonded at all coverages, and illustrates the drastic effect that atomic nitrogen has on the electronic structure of the W surface. Not only are there at least three types of chemisorbed hydrogen possible on the β-N-covered surface: molecular, on-top atomic, and distorted-bridge atomic, but the surface reactivity is enhanced towards hydrogen. The increased reactivity can be simply inferred by noting the small 0.7 L exposure which is needed to saturate the surface as compared to ~4 L in the case of clean W(100).

The observation of H chemisorption at the on-top site in the presence of β-N is just an example of an apparently general phenomenon inherent to this surface; chemisorption of one species can facilitate the on-top adsorption of a previously unallowed species. This behavior is also seen for the adsorption of on-top molecular αCO and γN in the presence of fourfold atomic β-CO (Ref. 50) and β-N,[51] respectively.

Beyond identification of a new type of H species, ir spectroscopy has allowed a probing of the interactions of on-top H with other adsorbed hydrogen as well as the metal surface itself and has established a paradigm of what can be expected for on-top adsorption in other systems. In particular, through-metal electronic coupling is still important in the dynamical interactions between the surface hydrogen with the magnitude of the interaction consistent with an estimation based solely on the areal density of surface lattice sites. While this estimation may be fortuitous, it does suggest that the exact adsorption location is of minor consequence in determining the strength of the coupling. Direct dipole-dipole interaction is also calculated to play a role in the interlayer dynamics.

Although interactions with the metal are obscured by inhomogeneous broadening of the line shape, the zero-coverage limit linewidth of 12 cm^{-1} is surprisingly narrow for a hydrogen mode. It is much sharper than typical transition-metal-surface–H symmetric-stretch modes which are in general significantly broader than typical EELS resolutions of 30–50 cm^{-1}, and is approximately half as narrow as the sharpest W_2H symmetric stretch of 20 cm^{-1} on clean W(100) which occurs at a coverage of 0.33 ML.[52]

The richness of H adsorption on this surface has also allowed the probing of static interactions between the on-top H and other chemisorbed hydrogen types. Perhaps most interesting is the large negative frequency shift caused by molecular coadsorption which suggests that chemisorbed H_2 is an electron donor to the metal surface. Additionally, it has been shown that gentle annealing of the 100-K exposed surface induces the top-bonded species to migrate to more tightly bound sites which inhibits further migration of the remaining on-top H.

Information on the underlying β-N layer has been gleaned from the W—H mode. A plateau in β-N island size of ~ 16 atoms for β-N coverages between 0.2 and 0.4 ML has been inferred. These observations are consistent with earlier LEED results at 0.4 ML.[12] For β-N coverages >0.5 ML a second ir line appears due to threefold coordination of the H by the β-N as opposed to solely twofold coordination at lower coverages.

This work has opened up interesting possibilities for future studies of nitrogen-hydrogen chemisorption on tungsten. Direct confirmation of more molecular D_2 compared with molecular H_2, perhaps with EELS or ir measurement of the internal stretch, would be satisfying. ir measurement of the N—H-stretch line shape for activated adsorption at higher temperatures might also prove fruitful, especially if other adsorbed species can be excluded so that inhomogeneous broadening can be minimized.

ACKNOWLEDGMENTS

One of us (D.M.R.) acknowledges stimulating conversations with W. P. Ambrose, S. P. Love, and L. J. Richter. Thanks also to Y. J. Chabal and D. C. Langreth for preprints of various papers. This work was supported by the National Science Foundation (NSF) under Grant No. DMR-87-14600 and by the U.S. Army Research Office (ARO) under Grant No. DAAL03-86-K-0103.

*Present address: AT&T Bell Laboratories, 600 Mountain Avenue, Murray Hill, NJ 07974-2070.

[1]See, e.g., the review article by K. Christmann, Surf. Sci. Rep. **9**, 1 (1988) and references therein. There is also evidence for a delocalized description of H chemisorption on some surfaces: see C. M. Mate and G. A. Somorjai, Phys. Rev. B **34**, 7417 (1986), and references therein.

[2]C. Nyberg and C. G. Tengstal, Phys. Rev. Lett. **50**, 1680 (1983).

[3]P. A. Karlsson, A. S. Martensson, S. Andersson, and P. Norlander, Surf. Sci. **175**, L759 (1986).

[4]L. J. Richter, T. A. Germer, J. P. Sethna, and W. Ho, Phys. Rev. B **38**, 10 403 (1988).

[5]See, e.g., K. Nakamoto, *Infrared and Raman Spectra of Inorganic and Coordination Compounds*, 3rd ed. (Wiley, New York, 1978).

[6]See U. A. Jayasooriya, M. A. Chesters, M. W. Howard, S. F. A. Kettle, D. B. Powell, and N. Sheppard, Surf. Sci. **93**, 526 (1980).

[7]There are many reviews on IRAS. See Y. J. Chabal, Surf. Sci. Rep. **8**, 211 (1988), and references therein.

[8]D. M. Riffe, L. M. Hanssen, A. J. Sievers, Y. J. Chabal, and S. B. Christman, Surf. Sci. **161**, L559 (1985).

[9]D. M. Riffe, L. M. Hanssen, and A. J. Sievers, Phys. Rev. B **34**, 692 (1986); Surf. Sci. **176**, 679 (1986).

[10]K. Yonehara and L. D. Schmidt, Surf. Sci. **92**, 201 (1980).

[11]D. L. Adams and L. H. Germer, Surf. Sci. **26**, 109 (1971).

[12]K. Griffiths, C. Kendon, D. A. King, and J. D. Pendry, Phys. Rev. Lett. **46**, 1584 (1981).

[13]W. Ho, R. F. Willis, and E. W. Plummer, Surf. Sci. **95**, 171 (1980).

[14]D. A. King and D. A. Wells, Proc. R. Soc. London, Ser. A **339**, 245 (1974).

[15]D. L. Adams and L. H. Germer, Surf. Sci. **27**, 21 (1971); S. Usami, N. Tominaga, and N. Nakajima, Vacuum **27**, 11 (1977); K. Griffiths and D. A. King, in *Proceedings of the Fourth International Conference on Solid Surfaces*, Suppl. No. 201 a la Revue *Le Vide, Les Couches Minces* (Société Française du Vide, Paris, 1980), p. 403.

[16]In Fig. 1, as well as throughout the rest of the paper, the reflectivity data are plotted as $\Delta R/R_0 = 1-(R/R_0)$ where R_0 is the reference reflectivity, taken before adsorption, and R is the reflectivity after adsorption. Hence, positive absorption corresponds to positive $\Delta R/R_0$. In addition, broadband changes in reflectivity are subtracted out using a linear interpolation between points away from the vibrational line of interest.

[17]Thermal-desorption areas were found unsatisfactory for determining the N_2 coverage presumably due to adsorption of N_2 gas onto surfaces nearby the sample which become warm, and thus desorb N_2, whenever the sample is heated.

[18]The TD areas in Fig. 3 were obtained by electron-bombardment heating of the sample from a tantalum filament suspended below the sample. All TD spectra above RT were produced in this manner since there is no simple way to otherwise heat the large crystal in a roughly linear fashion to high temperatures. The clean-surface β_1 and β_2 features, which are essentially identical to widely published curves, suggest that above-RT spectra are probably not very much affected by the e-beam current. Aside from the nonsample peak, below-RT spectra do not appear to be affected by the electron beam.

[19]See, e.g., P. W. Tamm and L. D. Schmidt, J. Chem. Phys. **52**, 1150 (1970).

[20]In the present vacuum system the decay constant of the pumps (~ 0.15 sec) is much faster than the time scale over which any of the TD features occur (~ 1 sec). Under these conditions the mass spectrometer current is proportional to the rate of the molecules thermally desorbing from the sample so that the area under the TD curve is proportional to the total amount desorbed from the surface.

[21]The heating rate affects the relative amounts of H_2 desorbed below RT ($\equiv$LT) and above RT ($\equiv$HT) especially in the broadband part between γ' and β_1'. The slower the rate, the more is desorbed below RT. The γ' areas in Fig. 4 and Table II are determined by assuming that the γ' peak is symmetric about its peak. The slightly lower γ' H_2 area in Fig. 4 com-

pared with Table II is due to a slightly faster LT heating rate (40 K/sec versus 32 K/sec) for the data in the figure which pushes the broadband LT part to higher temperatures. Also note that the γ' areas are not equal to that defined by "LT peak." See the discussion of Fig. 5 for further clarification.

[22]E. W. Plummer and A. E. Bell, J. Vac. Sci. Technol. **9**, 583 (1971).

[23]T. E. Madey, Surf. Sci. **29**, 571 (1972).

[24]The errors in $\int (R/R_0)dv$ quoted in this section for H_2, D_2, and HD adsorption are the errors associated with determining the correct baseline for the data in Fig. 6 which are from three runs taken only a short time apart, i.e., within 24 h of each other. On such a short time scale, ± 0.005 cm^{-1} is the error of the area of the W—H mode. On a longer time scale the drift in $\int (R/R_0)dv$ is slightly larger, due to drifts in the optical path. The best estimation on the actual integrated W—H area is 0.165 ± 0.010 cm^{-1}.

[25]J. D. E. McIntyre and D. E. Aspnes, Surf. Sci. **24**, 417 (1971).

[26]B. N. J. Persson and R. Ryberg, Phys. Rev. B **24**, 6954 (1981).

[27]Within reason—after reaching a given anneal temperature the area appears to quit changing in ~1–2 min. Waiting, e.g., 20 more minutes does not cause any more area to vanish.

[28]See, e.g., D. P. Woodruff, B. E. Hayden, K. Prince, and A. M. Bradshaw, Surf. Sci. **123**, 397 (1982).

[29]A. Adnot and J. D. Carette, Phys. Rev. Lett. **39**, 209 (1977).

[30]J. E. Reutt, Y. J. Chabal, and S. B. Christman, Phys. Rev. B **38**, 3112 (1988).

[31]For example, the W_2O symmetric stretch is at 742 cm^{-1} while the fourfold oxygen atom has a symmetric-stretch frequency of 605 cm^{-1}. See H. Frotzheim, H. Ibach, and S. Lehwald, Phys. Rev. B **14**, 1342 (1976).

[32]P. Norlander, S. Holloway, and J. K. Norskov, Surf. Sci. **136**, 59 (1984).

[33]F. M. Propst and T. C. Piper, J. Vac. Sci. Technol. **4**, 53 (1966). Such activated absorption is not expected to be a factor in this study. During adsorption an ion gauge is kept on to monitor the pressure, but its distance from the sample (~20 cm), the low exposures used (0.4 L), and relatively low temperature of the iridium-tungsten filament preclude this mode of adsorption as being important.

[34]M. P. Johnson and D. F. Shriver, J. Am. Chem. Soc. **88**, 301 (1966).

[35]H. Pfnur, D. Menzel, F. M. Hoffman, A. Ortega, and A. M. Bradshaw, Surf. Sci. **93**, 431 (1980).

[36]This number does depend slightly on the island shape and to a lesser extent on the distribution of island sizes about the average. For example, elongated islands (2×8) of 16 β-N atoms produce $\theta_f/\theta_{\beta\text{-N}} = 1.375$ compared to 1.5 for a 4×4 island.

[37]Y. J. Chabal, Phys. Rev. Lett. **55**, 845 (1985).

[38]M. Persson and B. Hellsing, Phys. Rev. Lett. **49**, 662 (1982); B. Hellsing, M. Persson, and B. I. Lunquist, Surf. Sci. **126**, 147 (1983); A. I. Volokitin, O. M. Braun, and V. M. Yakoulev, *ibid.* **172**, 31 (1986).

[39]Z. Y. Zhang and D. C. Langreth, Phys. Rev. B **39**, 10028 (1989).

[40]In the sequential H_2, D_2 experiment, the W—H frequency shifts from 1766 to 1755 cm^{-1}. However, approximately 19% of the on-top H is replaced by D so that this layer must be compared with an 81 at. % H–19 at. % D layer produced in the isotopic-mixture exposure experiments which exhibits a frequency of 1761 cm^{-1}. The resulting shift of $1755-1761 = -6$ cm^{-1} must then be scaled by the relative amounts of extra D_2 desorbed from a saturated D_2 layer beyond a saturated H_2 layer compared to the extra D_2 desorbed from the 1755-cm^{-1} layer beyond the 81 at. % H–19 at. % D isotopic layer. This correction (=1.3 which is obtained from Fig. 17) times -6 cm^{-1} finally yields a -8-cm^{-1} (saturation-molecular-D_2)–(saturation-molecular-H_2) chemical shift so that for the W—H stretch $\omega_{1,D_2} = 1758$ cm^{-1}.

[41]See, e.g., G. D. Mahan and A. A. Lucas, J. Chem. Phys. **68**, 1344 (1978); B. E. Hayden, K. Prince, D. P. woodruff, and A. M. Bradshaw, Phys. Rev. Lett. **51**, 475 (1983); and references therein for discussions of and expressions for the dipole sums.

[42]This number is estimated by assuming that the jellium edge is half the W interplane spacing parallel to the surface (0.8 Å) [see, e.g., E. Zaremba and W. Kohn, Phys. Rev. B **13**, 2270 (1976)] and that the jellium edge-image plane distance is 0.25 Å. [See J. A. Appelbaum and D. R. Hamann, Phys. Rev. B **6**, 1122 (1972).]

[43]L. W. Anders, R. S. Hansen, and L. S. Bartell, J. Chem. Phys. **59**, 5279 (1973).

[44]P. Norlander and S. Holstrom, Surf. Sci. **159**, 443 (1985).

[45]One might be tempted to also try and use data for the H symmetric stretch on clean W(100) to make an estimation for the on-top case presented here. There are at least three problems associated with this system. The first is that it is not clear how large the dynamical shifts are. EELS data and accompanying lattice dynamical calculations seem to indicate that the shifts should be ~48 cm^{-1} [see J. P. Woods, A. D. Kulkarni, J. L. Erskine, and F. W. de Wette, Phys. Rev. B **36**, 5848 (1987)] while ir data indicate a shift of only 20 cm^{-1} (see Ref. 37). Also for this system the hydrogen lattice is rotated 45° with respect to the underlying substrate atoms so that interactions are not along high-symmetry directions of the substrate as they are for the other cases at hand. The last problem is that for saturation H coverage on W(100) the adlattice constant (=2.23 Å) is small enough so that next-nearest-neighbor interactions are probably significant as opposed to the other four cases discussed.

[46]See, e.g., K. H. Lau and W. Kohn, Surf. Sci. **75**, 69 (1978); P. Johansson and H. Hjelmberg, *ibid.* **80**, 171 (1979); J. F. Dobson and G. H. Harris, Phys. Rev. B **27**, 6542 (1983).

[47]See N. W. Ashcroft and N. D. Mermin, *Solid State Physics* (Saunders College, Philadelphia, 1976), p. 36.

[48]Z. Schlesinger, L. H. Greene, and A. J. Sievers, Phys. Rev. B **32**, 2721 (1985).

[49]This follows simply from the EMT observation that the proton potential energy is a minimum at a certain surrounding electron density so that the restoring force is proportional to the gradient of the density about that point. See Ref. 44.

[50]See, e.g., H. Froitzheim, H. Ibach, and S. Lehwald, Surf. Sci. **63**, 56 (1977).

[51]D. M. Riffe, Ph.D. thesis, Cornell University, 1989 (unpublished).

[52]J. J. Arrecis, Y. J. Chabal, and S. B. Christman, Phys. Rev. B **33**, 7906 (1986).